Send Orders for Reprints to reprints@benthamscience.net

1428 *Anti-Cancer Agents in Medicinal Chemistry,* **2014**, *14,* **1428-1446**

Synthesis, Preferentially Hypoxic Apoptosis and Anti-Angiogenic Activity of 3-Amino-1,2,4-Benzotriazine-1,4-Dioxide Bearing Alkyl Linkers with a 3-Amino-1,2,4-Benzotriazine-1-Oxide Moiety

Chun-I Lee[1], Chien-Ming Huang[2,3], Wen-Hsin Huang[1,4,*] and An-Rong Lee[1,*]

[1]*Graduate Institute of Life Sciences, School and Institute of Pharmacy, National Defense Medical Center, No. 161, Section 6, Mingchuan E. Road, Taipei 11490, Taiwan;* [2]*Division of Pharmacy, Cheng-Hsin General Hospital, Taipei 11220, Taiwan;* [3]*Department of Nursing, Cardinal Tien College of Healthcare & Management, Taipei 23143, Taiwan and* [4]*Management Center, Department of Medical Research and Development, Show Chwan Health Care System, No. 6-1 Lukong Rd. Lugang, Changhua 50544, Taiwan*

Abstract: 3-(Aminoalkylamino)-1,2,4-benzotriazine-1,4-dioxide-extended derivatives were synthesized by the structural modification of 3-amino-1,2,4-benzotriazine-1,4-dioxide (tirapazamine, TPZ) that incorporated homologue-alkyl linkers, without or with an extended 3-amino-1,2,4-benzotriazine-1-oxide moiety at the 3-position of the TPZ. According to sequential evaluation of preferentially normoxic and hypoxic cytotoxicities against MCF-7, NCI-H460 and HCT-116, most of the synthesized compounds exhibited hypoxic cytotoxicity greater than or comparable to that of TPZ. Among them, compounds **9a** and **9b** more powerfully inhibited the proliferation of MCF-7, NCI-H460 and HCT-116 in hypoxia than did TPZ. The representative of 3-(aminoalkylamino)-1,2,4-benzotriazine-1,4-dioxide-extended derivatives, **9a** exhibited greater hypoxic cytotoxicity than TPZ, mediated by cell cycle arrest. The induction of DNA damage, the activation of caspase 3/7 and cleaved poly(ADP-ribose) polymerase-related apoptosis, which were detected in HCT-116 cells in both normoxia and hypoxia. *In vitro* anti-angiogenic assay of co-cultured HUVECs and fibroblasts that were exposed to the selected **7b**, **8g**, **9a** and **9b** exhibited 80-90% inhibition of tube formation at 20 μM, whereas TPZ exhibited approximately 50% inhibition of tube formation at 20 μM. At 2 μM, **9a** and **9b** significantly reduced the areas, lengths, paths and joints of tube formation by 70-80% and 45-50%, respectively. These results reveal that most of synthesized TPZ derivatives in this study exhibited more potent anti-angiogenesis than TPZ.

Keywords: Anti-angiogensis, apoptosis, 3-amino-1,2,4-benzotriazine-1,4-dioxide (tirapazamine), bioreductive agent, hypoxic cytotoxin.

1. INTRODUCTION

Bioreductive agents, a novel class of preferential cytotoxins in microenviromental hypoxia for the treatment of cancer, are effective remedies for solid tumors that are resistant to traditional chemotherapy and/or radiotherapy [1, 2].

In 1972, Sartorelli *et al.* [3] proposed evidence of the effectiveness of hypoxia-activated prodrugs as selectively bioreductive agents that are provided by cellular enzyme-catalyzed reductive activation to release active oxygen species (cytotoxins) localized inside hypoxic tumor cells, but may revert to ineffectiveness upon the re-oxygenation of cellular surroundings [3-5]. Tirapazamine (TPZ, 3-amino-1,2,4-benzotriazine-1,4-dioxide) (Fig. **1**) [6], an aromatic heterocyclic di-*N*-oxide, was firstly screened for herbicides in 1972 and described by Zeman *et al.* in 1986 as an originated and representative bioreductive agent such as mitomycin C with highly selective toxicity as a milestone development in cancer therapy [2].

TPZ, a bioreductive agent, is effectively reduced by cytochrome P450 and/or DT-diaphorase to release active cytotoxins at cellular micro-environmental hypoxia [6-8], which not only sequentially induces damage to DNA double-strands that involve an interaction with topoisomerase II, single-strand breakage, and even base-pair breakage, but also considerably promotes the covalent bonding of topoisomerase II to DNA that converts an inert kinetoplast DNA causing it to switch between its catenated and decatenated forms [9-20], resulting in cell apoptosis and increasing the effectiveness of chemotherapy and/or radiotherapy [7, 8].

TPZ, a hypoxia-selective cytotoxin, not only inhibits HIF-1α protein accumulation, especially in cellular deep hypoxia [12, 13], but also performs anti-angiogenesis in *in vitro* tests [14]. TPZ is undergoing an updated phase III cancer clinical trial, focusing on its combined use with cisplatin and radiation for treating advanced squamous cell carcinoma of the head and neck [21, 22].

While tirapazamine with limited effectiveness in anticancer trials has been reported [22], many investigations have shown that TPZ derivatives bearing extended moieties, such as alkyl or aromatic groups or heterocyclic chromophores at the 3-amino group targeting on DNA strands, have better activity and more hypoxic selectivity than TPZ [12-14, 23].

In this work, a series of 3-(aminoalkylamino)-1,2,4-benzotriazine-1,4-dioxide-extended derivatives that bear an alkyl linker with a heterocyclic 1,2,4-benzotriazine-1-oxide chromophore instead of 3-NH_2, introduced at the 3-position of TPZ, were synthesized in our laboratories. The cytotoxic activities of TPZ derivatives against MCF-7, NCI-H460 and HCT-116 in hypoxia and normoxia, respectively, were examined. After pre-screening of these TPZ derivatives, compounds **9a** and **9b** in comparison to TPZ for further *in vitro* biological and mechanism-elucidating investigations (elucidating the cell cycle, reactive oxygen species (ROS), caspase activity, and apoptosis) were assayed by flow cytometry in the HCT-116 cell line. An increasing number of studies have found that TPZ not only inhibits angiogenesis [12, 13] but also functions as a vascular targeting agent *in vitro* and *in vivo* in both normoxia and/or hypoxia [24-26]; therefore, some TPZ derivatives were also used to process anti-angiogenic assay.

*Address correspondence to these authors at the Graduate Institute of Life Sciences, School and Institute of Pharmacy, National Defense Medical Center, No. 161, Section 6, Mingchuan E. Road, Taipei 11490, Taiwan; Tel: +886-4-7813888#73631 (W. H. Huang); +886-2-87923100#18873 (A. R. Lee); Fax: +886-2-87923169; E-mails: wenhsin1495@gmail.com, wenhsin@ndmctsgh.edu.tw (W. H. Huang); lar@ndmctsgh.edu.tw (A. R. Lee)

1875-5992/14 $58.00+.00

2. MATERIALS AND METHODS

2.1. Chemical Synthesis

All chemical reagents (Sigma-Aldrich, Merck, Alfa Acros, Fluka and Showa) were used as received without further purification. TLC 60 F254 (Merck) was used for thin layer chromatography (TLC) and silica gel 60 (Merck, 70-230 mesh) was used for column chromatography. Infrared (IR) spectroscopy was performed by Perkin-Elmer 1600 series FT-IR Spectrophotometer. NMR spectra were recorded in DMSO-d_6 or acetic acid-d_4 at 300 or 400 MHz for ^{1}H by Varian GEMINI-300 or 400 FT-NMR Spectrometer (currently merged to Agilent Technologies), respectively.

Chemical shift (δ) was expressed as in parts per million (ppm) and the coupling constant (*J*) was reported in Hertz (Hz). These products were characterized by HRMS (Micromass® LCT Premier XE, currently merged to Waters Technologies) (positive mode, electrospray + ionization (ESI)).

Synthesis of Compounds 6

A solution of trifluoroacetic anhydride (10.5 g, 50.0 mmol) in dichloromethane (50.0 mL) was added dropwise to a solution of the respective diaminoalkanes (**4**, 100.0 mmol) and triethylamine (3.0 mL) in dichloromethane (20.0 mL) at -20 °C, and the mixture was stirred at 20 °C for 20 hrs. The mixture was partitioned between dichloromethane (100.0 mL) and water (25.0 mL). The organic layer was extracted with dichloromethane (2 × 100.0 mL) from the aqueous layer. The organic layer was evaporated to give the counterpart amine **5**. Compound **3** (3.0 g, 16.7 mmol) was added to a solution of amine **5** in ethanol (50.0 mL). The mixture was heated at reflux for 6 hrs. Solvent was evaporated and the residue was purified by chromatography to give the corresponding yellow solid compound **6** in 15 - 52 % yields.

Synthesis of N^n-{(1,4-Dioxido-1,2,4-benzotriazin-3-yl)aminoalkyl}-2,2,2,-trifluoroacetamides (7)

Hydrogen peroxide (30%, 6.2 mL, 60.0 mmol) was added dropwise to a stirring solution of trifluoroacetic anhydride (7.0 mL, 50.0 mmol) in dichloromethane (20.0 mL) at 0 °C and the mixture was stirred in 0 °C for 15 minutes. The solution was added to a solution of the respective trifluoroacetamides **6** (3.3 mmol) and trifluoroacetic acid (1.1 g, 10.0 mmol) in dichloromethane (20.0 mL). The reaction mixture was stirred at room temperature for 2 days and then the mixture cooled to 0 °C was slowly added to a cooled aqueous NH_3 solution. The mixture was extracted with dichloromethane (2 × 100.0 mL). The organic fraction was purified by chromatography to give the corresponding red solid compounds **7** (the yields ranged 29 - 50%) and counterpart precursor **6** (approx. 20 - 40 % recovery).

N^2-{(1,4-Dioxido-1,2,4-benzotriazin-3-yl)aminoethyl}-2,2,2,-trifluoroacetamide (7a)

Red solid (45% yield); mp 208-210 °C; IR (KBr) cm^{-1} 3246, 3010, 1716, 1620, 1602; ^{1}H-NMR (300 MHz, DMSO-d_6) δ 9.50 (s, 1H, -**NH**COCF$_3$), 8.47 (t, 1H, *J* = 6 Hz, Ar-**NH**-), 8.22 (dd, 1H, *J* = 8.4, 0.6 Hz, Ar-**H**), 8.14 (dd, 1H, *J* = 8.4, 0.6 Hz, Ar-**H**), 7.94 (ddd, 1H, *J* = 8.1, 7.5, 1.2 Hz, Ar-**H**), 7.58 (ddd, 1H, *J* = 8.1, 7.5, 1.2 Hz, Ar-**H**), 3.55 (q, 2H, *J* = 5.7 Hz, - NH**CH$_2$**CH$_2$NHCOCF$_3$), 3.45 (q, 2H, *J* = 5.6 Hz, -NHCH$_2$**CH$_2$**NHCOCF$_3$); ^{13}C-NMR (75 MHz, DMSO-d_6) δ 157.5, 157.0, 150.6, 138.9, 136.2, 130.7, 127.8, 121.8, 117.6, 41.0 - 39.2 (2 Cs overlap in solvent peak.); HRESI-MS: calcd., 317.0736 [M]$^+$, 318.0814 [M+H]$^+$; found, 318.0814 [M+H]$^+$, 340.0620 [M+Na]$^+$.

N^3-{(1,4-Dioxido-1,2,4-benzotriazin-3-yl)aminopropyl}-2,2,2-trifluoroacetamide (7b)

Red solid (33% yield); mp 204-205 °C; IR (KBr) cm^{-1} 3316, 3245, 3084, 1699, 1624, 1603; ^{1}H-NMR (300 MHz, DMSO-d_6) δ 9.44 (s, 1H, -**NH**COCF$_3$), 8.35 (t, 1H, *J* = 5.4 Hz, Ar-**NH**-), 8.19 (d, 1H, *J* = 8.4 Hz, Ar-**H**), 8.12 (d, 1H, *J* = 8.1 Hz, Ar-**H**), 7.92 (ddd, 1H, *J* = 7.8, 7.2, 1.2 Hz, Ar-**H**), 7.55 (ddd, 1H, *J* = 8.1, 7.7, 1.2 Hz, Ar-**H**), 3.56 (q, 2H, *J* = 6 Hz, -NH**CH$_2$**CH$_2$CH$_2$NHCOCF$_3$), 3.42 (q, 2H, *J* = 6.3 Hz, -NHCH$_2$CH$_2$**CH$_2$**NHCOCF$_3$), 1.82 (m, 2H, *J* = 6.6 Hz, - NHCH$_2$**CH$_2$**CH$_2$NHCOCF$_3$); ^{13}C-NMR (75 MHz, DMSO-d_6) δ 157.1, 156.7, 150.4, 138.8, 136.1, 130.6, 127.5, 121.7, 117.5, 38.5, 37.2, 28.1; HRESI-MS: calcd., 331.0892 [M]$^+$, 332.0970 [M+H]$^+$; found, 332.0974 [M+H]$^+$, 354.0796 [M+Na]$^+$.

N^4-{(1,4-Dioxido-1,2,4-benzotriazin-3-yl)aminobutyl}-2,2,2-trifluoroacetamide (7c)

This compound has been synthesized and published in early study [26]. Red solid (35% yield); mp 191-192 °C; IR (KBr) cm^{-1} 3251, 2360, 1701, 1625, 1602; ^{1}H-NMR (300 MHz, DMSO-d_6) δ 9.42 (s, 1H, -**NH**COCF$_3$), 8.35 (t, 1H, *J* = 6 Hz, Ar-**NH**-), 8.19 (d, 1H, *J* = 8.1 Hz, Ar-**H**), 8.11 (d, 1H, *J* = 8.1 Hz, Ar-**H**), 7.92 (ddd, 1H, *J* = 8.1, 7.7, 0.9 Hz, Ar-**H**), 7.54 (ddd, 1H, *J* = 8.1, 7.8, 1.2 Hz, Ar-**H**), 3.39 (t, 2H, *J* = 6.3 Hz, -NH**CH$_2$**CH$_2$CH$_2$CH$_2$NHCOCF$_3$), 3.20 (q, 2H, *J* = 6.3 Hz, -NHCH$_2$CH$_2$CH$_2$**CH$_2$**NHCOCF$_3$), 1.54 - 1.59 (m, 4H, -NHCH$_2$**CH$_2$CH$_2$**CH$_2$NHCOCF$_3$); ^{13}C-NMR (75 MHz, DMSO-d_6) δ 157.2, 156.8, 150.4, 138.8, 136.0, 127.4, 121.7, 117.4, 40.8 - 39.2 (2 Cs overlap in solvent peak.), 26.3, 25.9; HRESI-MS: calcd., 345.1049 [M]$^+$, 346.1127 [M+H]$^+$; found, 346.1136 [M+H]$^+$, 368.0949 [M+Na]$^+$.

N^5-{(1,4-Dioxido-1,2,4-benzotriazin-3-yl)aminopentyl}-2,2,2-trifluoroacetamide (7d)

This compound has been synthesized and published in early study [27]. Red solid (50% yield); mp 195-197 °C; IR (KBr) cm^{-1} 3265, 3105, 2943, 1700, 1633; ^{1}H-NMR (300 MHz, DMSO-d_6) δ 9.40 (s, 1H, -**NH**COCF$_3$), 8.31 (t, 1H, *J* = 6 Hz, Ar-**NH**-), 8.18 (d, 1H, *J* = 6 Hz, Ar-**H**), 8.11 (d, 1H, *J* = 8.7 Hz, Ar-**H**), 7.91 (ddd, 1H, *J* = 8.0, 7.8, 0.9 Hz, Ar-**H**), 7.54 (ddd, 1H, *J* = 8.0, 7.8, 0.9 Hz, Ar-**H**), 3.37 (q, 2H, *J* = 6.9 Hz, -NH**CH$_2$**CH$_2$CH$_2$CH$_2$CH$_2$NHCOCF$_3$), 3.17 (q, 2H, *J* = 6.6 Hz, -NHCH$_2$CH$_2$CH$_2$CH$_2$**CH$_2$**NHCOCF$_3$), 1.28 - 1.66 (m, 6H, -NHCH$_2$**CH$_2$CH$_2$CH$_2$**CH$_2$NHCOCF$_3$); ^{13}C-NMR (75 MHz, DMSO-d_6) δ 157.5, 157.0, 150.6, 138.9, 136.1, 130.6, 127.6, 121.8, 117.5, 40.8 - 39.2 (2 Cs overlap in solvent peak.), 28.8, 28.4, 24.0; HRESI-MS: calcd., 359.1205 [M]$^+$, 360.1283 [M+H]$^+$; found, 360.1285 [M+H]$^+$, 382.1109 [M+Na]$^+$.

N^6-{(1,4-Dioxido-1,2,4-benzotriazin-3-yl)aminohexyl}-2,2,2,-trifluoroacetamide (7e)

This compound has been synthesized and published in early patent [28]. Red solid (31% yield); mp 160-161 °C; IR (KBr) cm^{-1} 3252, 2359, 1700, 1624, 1602; ^{1}H-NMR (300 MHz, DMSO-d_6) δ 9.40 (s, 1H, -**NH**COCF$_3$), 8.31 (s, 1H, Ar-**NH**-), 8.18 (dd, 1H, *J* = 8.6, 0.3 Hz, Ar-**H**), 8.10 (d, 1H, *J* = 8.7 Hz, Ar-**H**), 7.91 (ddd, 1H, *J* = 8.1, 7.8, 1.2 Hz, Ar-**H**), 7.53 (ddd, 1H, *J* = 8.1, 7.8, 1.2 Hz, Ar-**H**), 3.37 (q, 2H, *J* = 6.9 Hz, -NH**CH$_2$**CH$_2$CH$_2$CH$_2$CH$_2$CH$_2$NHCOCF$_3$), 3.16 (q, 2H, *J* = 6.8 Hz, -NHCH$_2$CH$_2$CH$_2$CH$_2$CH$_2$**CH$_2$**NHCOCF$_3$), 1.30 - 1.62 (m, 8H, -NHCH$_2$**CH$_2$CH$_2$CH$_2$CH$_2$**CH$_2$NH-COCF$_3$); ^{13}C-NMR (75 MHz, DMSO-d_6) δ 157.5, 157.0, 150.6, 138.9, 136.1, 130.6, 127.5, 121.8, 117.6, 41.2 - 39.2 (2 Cs overlap in solvent peak.), 29.1, 28.7, 26.4, 26.3; HRESI-MS: calcd., 373.1362 [M]$^+$, 374.1440 [M+H]$^+$; found, 374.1453 [M+H]$^+$, 396.1268 [M+Na]$^+$.

N^7-{(1,4-Dioxido-1,2,4-benzotriazin-3-yl)aminoheptyl}-2,2,2-trifluoroacetamide (7f)

Red solid (29% yield); mp 143-145 °C; IR (KBr) cm^{-1} 3250, 1695, 1625, 1602; ^{1}H-NMR (300 MHz, DMSO-d_6) δ 9.39 (s, 1H, -**NH**COCF$_3$), 8.31 (t, 1H, *J* = 6.3 Hz, Ar-**NH**-), 8.17 (d, 1H, *J* = 8.4 Hz, Ar-**H**), 8.10 (d, 1H, *J* = 8.1 Hz, Ar-**H**), 7.90 (t, 1H, *J* = 7.2 Hz, Ar-**H**), 7.53 (t, 1H, *J* = 7.4 Hz, Ar-**H**), 3.38 - 3.40 (2 Hs overlap in

solvent peak, -NH**CH$_2$**CH$_2$CH$_2$CH$_2$CH$_2$CH$_2$NHCOCF$_3$), 3.15 (q, 2H, *J* = 6.6 Hz, -NHCH$_2$CH$_2$CH$_2$CH$_2$CH$_2$CH$_2$**CH$_2$**NHCOCF$_3$), 1.20 - 1.59 (m, 10H, - NHCH$_2$**CH$_2$CH$_2$CH$_2$CH$_2$CH$_2$**CH$_2$NHCOCF$_3$); 1H-NMR (300 MHz, CD_3COOD) δ 8.32 (d, 1H, *J* = 8.4 Hz, Ar-**H**), 8.21 (d, 1H, *J* = 7.8 Hz, Ar-**H**), 8.00 (s, 1H, Ar-**H**), 7.57 (t, 1H, *J* = 7.4 Hz, Ar-**H**), 3.60 (s, 2H, -NH**CH$_2$**CH$_2$CH$_2$CH$_2$CH$_2$CH$_2$ CH$_2$NHCOCF$_3$), 3.50 (t, 2H, *J* = 7.1 -NHCH$_2$CH$_2$CH$_2$CH$_2$CH$_2$CH$_2$ **CH$_2$**NHCOCF$_3$), 1.72 (s, 2H, -NHCH$_2$**CH$_2$**CH$_2$CH$_2$CH$_2$CH$_2$CH$_2$ NHCOCF$_3$), 1.60 (s, 2H, -NHCH$_2$CH$_2$CH$_2$CH$_2$CH$_2$**CH$_2$**CH$_2$ NHCOCF$_3$), 1.30 (s, 6H, - NHCH$_2$CH$_2$**CH$_2$CH$_2$CH$_2$**CH$_2$CH$_2$ NHCOCF$_3$); ^{13}C-NMR (75 MHz, DMSO-*d*$_6$) δ 157.8, 157.2, 150.6, 138.9, 136.5, 130.7, 127.8, 121.9, 117.6, 41.3 - 39.2 (2 Cs overlap in solvent peak.), 29.2, 28.8, 28.7, 26.7 (2C); ^{13}C-NMR (75 MHz, acetic acid-*d*$_4$) δ 151.8, 139.8, 138.7, 132.4, 128.2, 122.7, 117.8, 42.4, 40.9, 29.9, 29.7, 29.5, 2 7.5, 27.3; HRESI-MS: calcd., 387.1518 $[M]^+$, 388.1596 $[M+H]^+$; found, 388.1603 $[M+H]^+$, 410.1416 $[M+Na]^+$.

N^8-{(1,4-Dioxido-1,2,4-benzotriazin-3-yl)aminooctyl}-2,2,2,-trifluoroacetamide (7g)

Red solid (32% yield); mp 156-158 °C; IR (KBr) cm^{-1} 3281,2926,1697,1604; ^{1}H-NMR (300 MHz, DMSO-*d*$_6$) δ 9.40 (s, 1H, -**NH**COCF$_3$), 8.33 (t, 1H, *J* = 6.3 Hz, Ar-**NH**-), 8.18 (d, 1H, *J* = 8.4 Hz, Ar-**H**), 8.11 (d, 1H, *J* = 8.1 Hz, Ar-**H**), 7.91 (t, 1H, *J* = 7.2 Hz, Ar-**H**), 7.53 (t, 1H, *J* = 7.4 Hz, Ar-**H**), 3.30 - 3.45(2H, -NH**CH$_2$**CH$_2$CH$_2$CH$_2$CH$_2$CH$_2$NHCOCF$_3$, overlap in H_2O.), 3.15 (q, 2H, *J* = 6.6 Hz, -NHCH$_2$CH$_2$-CH$_2$CH$_2$CH$_2$CH$_2$**CH$_2$** NHCOCF$_3$), 1.59 (t, 2H, *J* = 6.3, Hz -NHCH$_2$**CH$_2$**CH$_2$CH$_2$CH$_2$CH$_2$ CH$_2$NHCOCF$_3$), 1.45 (t, 2H, *J* = 6.5 Hz, -NHCH$_2$CH$_2$CH$_2$CH$_2$CH$_2$ **CH$_2$**-CH$_2$NHCOCF$_3$), 1.22 (s, 4H, -NHCH$_2$CH$_2$CH$_2$**CH$_2$CH$_2$**CH$_2$ CH$_2$NHCOCF$_3$); ^{13}C-NMR (75 MHz, DMSO-*d*$_6$) δ 157.5, 157.1, 150.6, 138.9, 136.1, 130.6, 127.5, 121.8, 117.5, 41.3 - 39.3 (2 Cs overlap in solvent peak.), 29.2, 29.1, 29.0, 28.7, 26.7, 26.6; HRESI-MS: calcd., 401.1675 $[M]^+$, 402.1753 $[M+H]^+$; found, 402.1774 $[M+H]^+$, 424.1585 $[M+Na]^+$.

Synthesis of N^1-(1,4-Dioxido-1,2,4-benzotriazine-3-yl)-alkanediamines (8)

Aqueous NH_3 (10.0 mL) was added to a solution of dioxide **7** in methanol (10.0 mL) and the mixture stirred at room temperature for 24 hrs. The solvent was evaporated and afforded red solid compound **8** (quant. ~ 99% yield).

N^1-(1,4-Dioxido-1,2,4-benzotriazine-3-yl)-1,2-ethanediamine (8a)

Red solid (quant.); mp 175-178 °C; IR (KBr) cm^{-1} 3452, 3235, 3095, 1683, 1619; ^{1}H-NMR (300 MHz, DMSO-*d*$_6$) δ 8.23 (d, 1H, *J* = 8.7 Hz, Ar-**H**), 8.16 (d, 1H, *J* = 8.4 Hz, Ar-**H**), 7.96 (t, 1H, *J* = 7.8 Hz, Ar-**H**), 7.60 (t, 1H, *J* = 7.8 Hz, Ar-**H**), 3.66 (t, 2H, *J* = 5.9 Hz, -NH**CH$_2$**CH$_2$NH$_2$), 3.07 (t, 2H, *J* = 6 Hz, -NHCH$_2$**CH$_2$**NH$_2$); ^{13}C-NMR (75 MHz, DMSO-*d*$_6$) δ 150.5, 138.7, 136.1, 130.7, 127.9, 121.5, 117.5, 40.8 - 38.8 (2 Cs overlap in solvent peak.); HRESI-MS: calcd., 221.0913 $[M]^+$, 222.0991 $[M+H]^+$; found, 222.0981 $[M+H]^+$, 244.0798 $[M+Na]^+$.

N^1-(1,4-Dioxido-1,2,4-benzotriazine-3-yl)-1,3-propanediamine (8b)

This compound has been synthesized and published in early patent [28]. Red solid (quant.); mp 160-162 °C; IR (KBr) cm^{-1} 3460, 3358, 3050, 2363, 1678, 1615, 1594; ^{1}H-NMR (300 MHz, DMSO-*d*$_6$) δ 8.40 (s, 1H, Ar-**NH**-), 8.20 (d, 1H, *J* = 7.8 Hz, Ar-**H**), 8.13 (d, 1H, *J* = 8.1 Hz, Ar-**H**), 7.94 (ddd, 1H, *J* = 8.1 ,7.5, 1.2 Hz, Ar-**H**), 7.76 (s, 2H, **-NH$_2$**), 7.57 (ddd, 1H, *J* = 7.8, 7.2, 1.2 Hz, Ar-**H**), 3.47 (d, 2H, *J* = 2.7 Hz, -NH**CH$_2$**CH$_2$CH$_2$NH$_2$), 2.88 (t, 2H, *J* = 7.5 Hz, - NHCH$_2$CH$_2$**CH$_2$**NH$_2$), 1.90 (m, 2H, -NHCH$_2$**CH$_2$** CH$_2$NH$_2$); ^{13}C-NMR (75 MHz, DMSO-*d*$_6$) δ 154.4, 142.7, 139.9, 134.5, 131.6, 125.5, 121.4, 42.2, 41.0, 30.9; HRESI-MS: calcd., 235.1069 $[M]^+$, 236.1147 $[M+H]^+$; found, 236.1137 $[M+H]^+$, 258.0959 $[M+Na]^+$.

N^1-(1,4-Dioxido-1,2,4-benzotriazine-3-yl)butyl]-1,4-butanediamine (8c)

This compound has been synthesized and published in early study [27]. Red solid (quant.); mp 161-163 °C; IR (KBr) cm^{-1} 3440, 3246, 3092, 2969, 2359; ^{1}H-NMR (300 MHz, DMSO-*d*$_6$) δ 8.39 (s, 1H, Ar-**NH**-), 8.20 (d, 1H, *J* = 8.7 Hz, Ar-**H**), 8.13 (dd, 1H, *J* = 8.4, 0.6 Hz, Ar-**H**), 7.93 (ddd, 1H, *J* = 8.1 ,7.7, 1.5 Hz, Ar-**H**), 7.67 (s, 2H, **-NH$_2$**), 7.56 (ddd, 1H, *J* = 8.1, 7.7, 0.9 Hz, Ar-**H**), 3.32 - 3.41 (2 Hs ovelap in solvent peak, -NH**CH$_2$**CH$_2$CH$_2$CH$_2$NH$_2$), 2.82 (t, 2H, *J* = 7.2 Hz, -NHCH$_2$CH$_2$CH$_2$**CH$_2$**NH$_2$), 1.56 - 1.67 (m, 4H, -NHCH$_2$**CH$_2$CH$_2$**CH$_2$CH$_2$NH$_2$); ^{13}C-NMR (75 MHz, DMSO-*d*$_6$) δ 150.5, 138.6, 136.9, 130.5, 127.5, 121.7, 117.5, 40.8 - 39.0 (2 Cs overlap in solvent peak.), 25.9, 24.7; HRESI-MS: calcd., 249.1226 $[M]^+$, 250.1304 $[M+H]^+$; found, 250.1302 $[M+H]^+$, 272.1119 $[M+Na]^+$.

N^1-(1,4-Dioxido-1,2,4-benzotriazine-3-yl)-1,5-pentanediamine (8d)

This compound has been synthesized and published in early study [27]. Red solid (quant.); mp 152-154 °C; IR (KBr, cm^{-1}) 3432, 3249, 2943, 2364, 1684, 1621 ; 1H-NMR (300 MHz, DMSO-*d*$_6$) δ 8.33 (s, 1H, Ar-**NH**-), 8.19 (d, 1H, *J* = 8.4 Hz, Ar-**H**), 8.12 (d, 1H, *J* = 8.1 Hz, Ar-**H**), 7.93 (t, 1H, *J* = 7.8 Hz, Ar-**H**), 7.69 (s, 2H, **-NH$_2$**), 7.55 (t, 1H, *J* = 7.4 Hz, Ar-**H**), 3.31 - 3.37 (2 Hs ovelap in solvent peak, -NH**CH$_2$**CH$_2$CH$_2$CH$_2$CH$_2$NH$_2$), 2.78 (t, 2H, *J* = 7.5 Hz, -NHCH$_2$CH$_2$CH$_2$CH$_2$**CH$_2$**NH$_2$), 1.53 - 1.64 (m, 4H, -NHCH$_2$ **CH$_2$**CH$_2$**CH$_2$**CH$_2$NH$_2$), 1.37 (q, 2H, *J* = 8.7 Hz, -NHCH$_2$CH$_2$**CH$_2$** CH$_2$CH$_2$-NH$_2$); ^{13}C-NMR (75 MHz, DMSO-*d*$_6$) δ 150.5, 138.8, 136.1, 130.5, 127.5, 121.6, 117.4, 40.8 - 39.2 (2 Cs overlap in solvent peak.), 28.5, 27.1, 23.5; HRESI-MS: calcd., 263.1382 $[M]^+$, 264.1460 $[M+H]^+$; found, 264.1457 $[M+H]^+$, 286.1271 $[M+Na]^+$.

N^1-(1,4-Dioxido-1,2,4-benzotriazin-3-yl)-1,6-hexanediamine (8e)

This compound has been synthesized and published in early study [16]. Red solid (quant.); mp 131-135 °C; IR (KBr) cm^{-1} 3436, 3234, 3099, 2938, 2845, 1699, 1618, 1600; ^{1}H-NMR (300 MHz, DMSO-*d*$_6$) δ 8.31 (s, 1H, Ar-**NH**-), 8.18 (d, 1H, *J* = 8.7 Hz, Ar-**H**), 8.10 (d, 1H, *J* = 8.7 Hz, Ar-**H**), 7.91 (ddd, 1H, *J* = 7.8, 7.2, 1.2 Hz, Ar-**H**), 7.73 (s, 2H, **-NH$_2$**), 7.54 (t, 1H, *J* = 8.1 Hz, Ar-**H**), 3.15 (s, 2H, -NH**CH$_2$**CH$_2$CH$_2$CH$_2$CH$_2$CH$_2$NH$_2$), 2.77 (t, 2H, *J* = 7.5 Hz, -NHCH$_2$CH$_2$CH$_2$CH$_2$CH$_2$**CH$_2$**NH$_2$), 1.32 - 1.62 (m, 8H, -NHCH$_2$ **CH$_2$CH$_2$CH$_2$CH$_2$**CH$_2$NH$_2$); ^{13}C-NMR (75 MHz, DMSO-*d*$_6$) δ 150.4, 138.8, 136.0, 130.4, 127.4, 121.6, 117.4, 41.0 - 39.2 (2 Cs overlap in solvent peak.), 28.9, 27.3, 26.9, 25.8; ^{13}C-NMR (75 MHz, acetic acid-*d*$_4$) δ 151.8, 139.7, 138.7, 132.4, 128.3, 122.6, 117.8, 42.3, 41.8, 29.7, 28.0, 26.9, 26.8; HRESI-MS: calcd., 277.1539 $[M]^+$, 278.1617 $[M+H]^+$; found, 278.1618 $[M+H]^+$, 300.1427 $[M+Na]^+$.

N^1-(1,4-Dioxido-1,2,4-benzotriazine-3-yl)-1,7-heptanediamine (8f)

Red solid (quant.); mp 170-173 °C; IR (KBr) cm^{-1} 3257, 2936, 2859, 1675, 1623, 1598; ^{1}H-NMR (300 MHz, DMSO-*d*$_6$) δ 8.27 (s, 1H, Ar-**NH**-), 8.19 (d, 1H, *J* = 8.7 Hz, Ar-**H**), 8.11 (d, 1H, *J* = 8.7 Hz, Ar-**H**), 7.92 (ddd, 1H, *J* = 7.5, 7.2, 1.2 Hz, Ar-**H**), 7.75 (s, 2H, **-NH$_2$**), 7.55 (ddd, 1H, *J* = 7.5, 7.2, 1.2 Hz, Ar-**H**), 3.35 (2 Hs overlap in solvent peak, -NH**CH$_2$**CH$_2$CH$_2$CH$_2$CH$_2$CH$_2$NH$_2$), 2.76 (t, 2H, *J* = 7.5 Hz, -NHCH$_2$CH$_2$CH$_2$CH$_2$CH$_2$CH$_2$**CH$_2$**NH$_2$), 1.30 - 1.60 (m, 10H, -NHCH$_2$**CH$_2$CH$_2$CH$_2$CH$_2$CH$_2$**CH$_2$NH$_2$); ^{1}H-NMR (300 MHz, CD_3COOD-*d*$_4$) δ 8.32 (d, 1H, *J* = 8.1 Hz, H-9), 8.20 (d, 1H, *J* = 8.1 Hz, H-6), 8.01 (t, 1H, *J* = 7.5 Hz, H-8), 7.58 (t, 1H, *J* = 7.5, 7.8 Hz, H-7), 3.59 (t, 2H, *J* = 6.8 Hz, -NH**CH$_2$** CH$_2$CH$_2$CH$_2$CH$_2$CH$_2$CH$_2$NH$_2$), 3.08 (t, 2H, *J* = 6.8 Hz, -NHCH$_2$ CH$_2$CH$_2$CH$_2$CH$_2$CH$_2$**CH$_2$**.NH$_2$), 1.73 (s, 4H, -NHCH$_2$**CH$_2$**CH$_2$CH$_2$ CH$_2$**CH$_2$**CH$_2$NH$_2$), 1.42 (s, 4H, -NHCH$_2$CH$_2$**CH$_2$CH$_2$CH$_2$**CH$_2$ CH$_2$NH$_2$); ^{13}C-NMR (75 MHz, CD_3COOD-*d*$_4$) δ 151.8, 139.7, 138.7, 132.4, 128.3, 122.6, 117.8, 42.4, 41.1, 29.8, 29.5, 28.0, 27.2, 27.1; ^{13}C-NMR (75 MHz, DMSO-*d*$_6$) δ 150.4, 138.7, 135.9,

130.4, 127.4, 121.5, 117.3, 41.0, (one carbon peak overlap in solvent peak in 42 – 39.), 28.9, 28.4, 27.2, 26.3, 26.0; HRESI-MS: calcd., 291.1695 $[M]^+$, 292.1773 $[M+H]^+$; found, 292.1762 $[M+H]^+$.

N^1-(1,4-Dioxido-1,2,4-benzotriazine-3-yl)-1,8-octanediamine (8g)

Red solid (quant.); mp 141-145 °C; IR (KBr) cm^{-1} 3431, 3270, 2921, 2852, 1704, 1599; ^{1}H-NMR (300 MHz, DMSO-d_6) δ 8.31 (s, 1H, Ar-**NH**-), 8.19 (d, 1H, *J* = 9 Hz, Ar-**H**), 8.11 (d, 1H, *J* = 8.7 Hz, Ar-**H**), 7.92 (t, 1H, *J* = 6.9 Hz, Ar-**H**), 7.64 (s, 2H, **-NH_2**), 7.54 (ddd, 1H, *J* = 8.4, 8.0, 1.5 Hz, Ar-**H**), 3.30 - 3.38 (2 Hs overlap in solvent peak, -NH**CH_2**$CH_2CH_2CH_2CH_2CH_2CH_2NH_2$), 2.75 (t, 2H, *J* = 7.7 Hz, -$NHCH_2CH_2$-$CH_2CH_2CH_2CH_2CH_2$**CH_2**NH_2), 1.28 - 1.60 (m, 12H, -$NHCH_2$**$CH_2CH_2CH_2CH_2CH_2$**-**CH_2**CH_2NH_2); ^{1}H-NMR (300 MHz, CD_3COOD-d_4) δ 8.32 (d, 1H, *J* = 8.7 Hz, H-9), 8.20 (d, 1H, *J* = 9 Hz, H-6), 8.00 (t, 1H, *J* = 7.5 Hz, H-8), 7.57 (t, 1H, *J* = 8.1, 1.5 Hz, H-7), 3.59 (t, 2H, *J* = 7.1 Hz, -NH**CH_2**CH_2 $CH_2CH_2CH_2CH_2CH_2CH_2NH_2$), 3.07 (t, 2H, *J* = 7.5 Hz, -$NHCH_2$ $CH_2CH_2CH_2CH_2$-CH_2CH_2**CH_2**NH_2), 1.72 (s, 4H, -$NHCH_2$**CH_2**CH_2 $CH_2CH_2CH_2$**CH_2**CH_2NH_2), 1.39 (s, 8H, - $NHCH_2CH_2$**$CH_2CH_2CH_2$** **CH_2**$CH_2CH_2NH_2$); ^{13}C-NMR (75 MHz, CD_3COOD-d_4) δ 151.8, 139.8, 138.7, 132.4, 128.3, 122.7, 117.8, 42.5, 41.2, 30.0, 29.8 (2), 28.9, 27.4, 27.1; HRESI-MS: calcd., 305.1852 $[M]^+$, 306.1930 $[M+H]^+$. found, 306.1934 $[M+H]^+$.

Synthesis of N^1-(1-Oxido-1,2,4-benzotriazin-3-yl)-N^n-(1-dioxido-1,2,4-benzotriazin-3-yl)-1,n-alkyl-diamines (9)

Compound **3** (0.8 g, 4.1 mmol) was added to a solution of the respective compound **8** (4.1 mmol) in methanol (20.0 mL) and triethylamine (0.6 mL) and the mixture was heated at reflux for 10 hrs. The mixture was added to a solution of 20 ml of propanol and triethylamine (5.0 mL). The solvent was evaporated and the residue was purified by hot ethanol to give the corresponding red solid compound **9** (14 - 45%).

3-(2-[(1-Oxido-1,2,4-benzotriazin-3-yl)amino]ethylamino)-1,2,4-benzotriazine-1,4-dioxide (9a)

Red solid (35% yield); mp 213-215 °C; IR (KBr, cm^{-1}) 3448, 2362, 1616; ^{1}H-NMR (300 MHz, DMSO-d_6) δ 8.47 (s, 1H, Ar-**NH**-), 8.20 (d, 1H, *J* = 7.8 Hz, Ar-**H**), 8.10 (dd, 2H, *J* = 10.8, 9.6 Hz, Ar-**H**), 7.98 (s, 1H, Ar-**NH**-), 7.92 (dd and dd, 1H, *J* = 4.5,1.2, and 5.7, 1.5 Hz, Ar-**H**), 7.73 (t, 1H, *J* = 6.9, Ar-**H**) 7.56 (dd and dd, 1H, *J* = 8.1, 1.2, and 7.8, 1.2 Hz, Ar-**H**), 7.48 (d, 1H, *J* = 6 Hz, Ar-**H**), 7.32 (dd and dd, 1H *J* = 6.9, 1.2, and 8.1, 1.2 Hz, Ar-**H**), 3.63 - 3.66 (m, 4H, -NH**CH_2CH_2**NH-); ^{13}C-NMR (75 MHz, DMSO-d_6) δ 159.7, 150.6, 149.0, 138.7, 136.1, 135.9, 130.7, 130.5, 127.5, 126.5, 125.1, 121.5, 120.3, 117.3, 40.8 - 39.2 (2 Cs overlap in solvent peak.); HRESI-MS: calcd., 366.1189 $[M]^+$, 367.1267 $[M+H]^+$; found, 367.1277 $[M+H]^+$, 389.1097 $[M+Na]^+$.

3-(3-[(1-Oxido-1,2,4-benzotriazin-3-yl)amino]propylamino)-1,2,4-benzotriazine-1,4-dioxide (9b)

Red solid (17% yield); mp 203-204 °C; IR (KBr, cm^{-1}) 3288, 1610,1590; ^{1}H-NMR (300 MHz, DMSO-d_6) δ 8.43 (s, 1H, Ar-**NH**-), 8.09 - 8.15 (m, 3H, Ar-**H**), 7.89 - 7.94 (m, 2H, Ar-**H**), 7.69 (t, 1H, *J* = 8.1, Ar-**H**), 7.49 - 7.56 (m, 2H, Ar-**H** and Ar-**NH**-), 7.29 (dd and dd, 1H, *J* = 8.4, 1.2, and 7.2, 1.2 Hz, Ar-**H**), 3.42 - 3.55 (overlap in solvent peak, m, 4H, - NH**CH_2**CH_2**CH_2**NH-), 1.91 (t, 2H, *J* = 6.5 Hz, -$NHCH_2$**CH_2**CH_2NH-); ^{13}C-NMR (75 MHz, DMSO-d_6) δ 159.9, 150.6, 149.0, 138.9, 136.2, 136.1, 130.8, 130.6, 127.6, 126.6, 125.1, 121.7, 120.5, 117.6, 38.7, 38.2, 28.8; HRESI -MS: calcd., 380.1345 $[M]^+$, 381.1424 $[M+H]^+$; found, 381.1443 $[M+H]^+$, 403.1251 $[M+Na]^+$.

3-(4-[(1-Oxido-1,2,4-benzotriazin-1-ium-3-yl)amino]butylamino)-1,2,4-benzotriazine-1,4-dioxide (9c)

Red solid (15% yield); mp 207-210 °C; IR (KBr, cm^{-1}) 3315, 3246, 3098, 2928, 1587; ^{1}H-NMR (400 MHz, DMSO-d_6) δ 8.32 (s, 1H, Ar-**NH**-), 8.18 (d, 1H, *J* = 8.0, Ar-**H**), 8.1 - 8.12 (m, 2H, Ar-**H**), 7.91 - 7.94 (m, 2H, Ar-**H** and Ar-**NH**), 7.75 (t, 1H, *J*=8, Ar-**H**), 7.52 - 7.54 (m, 2H, Ar-**H**), 7.29 (t, 1H, *J* = 8 Hz, Ar-**H**), 3.42 - 3.55 (overlap in solvent peak, m, 4H, -NH**CH_2**CH_2CH_2**CH_2**NH-), 1.67 (m, 4H, -$NHCH_2$**CH_2CH_2**CH_2NH-); ^{13}C-NMR (100 MHz, DMSO-d_6) δ 159.8, 150.5, 149.2, 138.7, 136.2, 135.9, 130.5, 130.4, 127.3, 126.5, 124.9, 121.6, 120.4, 117.3, 41.1 - 39.2 (2 Cs overlap in solvent peak.), 29.5, 29.4. HRESI-MS: calcd., 394.1631 $[M]^+$, 395.1580 $[M+H]^+$; found, 395.1574 $[M+H]^+$.

3-(5-[(1-Oxido-1,2,4-benzotriazin-1-ium-3-yl)amino]pentylamino)-1,2,4-benzotriazine-1,4-dioxide (9d)

Red solid (14% yield); mp 213-214 °C; IR (KBr, cm^{-1}) 3315, 3246, 3098, 2928, 1587; ^{1}H-NMR (300 MHz, acetic acid-d_4) δ 8.32 (d, 1H, *J* = 9, Ar-**H**), 8.20 - 8.22 (m, 2H, Ar-**H**), 8.00 (t, 1H, *J* = 6, Ar-**H**), 7.75 (t, 1H, *J* = 6.6, Ar-**H**), 7.55 - 7.59 (m, 2H, Ar-**H**), 7.32 (t, 1H, *J* = 6.6, Ar-**H**), 3.43 - 3.56 (m, 4H, -NH**$CH_2CH_2CH_2CH_2$** **CH_2**NH-), 1.55 - 1.80 (m, 6H, -$NHCH_2$**$CH_2CH_2CH_2$**CH_2NH-); ^{13}C-NMR (75 MHz, acetic acid-d_4) δ 160.1, 152.0, 139.8, 138.6, 137.4, 132.4, 128.2, 126.2, 122.7, 121.7, 117.8, 42.4, 42.1, 29.7 (2 Cs), 24.8; HRESI-MS: calcd., 408.1658 $[M]^+$, 409.1737 $[M+H]^+$; found, 409.1759 $[M+H]^+$, 431.1565 $[M+Na]^+$.

3-(6-[(1-Oxido-1,2,4-benzotriazin-1-ium-3-yl)amino]hexylamino)-1,2,4-benzotriazine-1,4-dioxide (9e)

Red solid (37% yield); mp 230-233 °C; IR (KBr, cm^{-1}) 3290, 2929, 2851, 1710, 1593, 1568; ^{1}H-NMR (300 MHz, DMSO-d_6) δ 8.32 (s, 1H, Ar-**NH**-), 8.18 (d, *J* = 6, 1H, Ar-**H**), 8.10 - 8.12 (m, 2H, Ar-**H**), 7.89 - 7.83 (m, 2H, Ar-**H** and Ar-**NH**-), 7.73 (t, 1H, *J* = 6.0, Ar-**H**), 7.54 - 7.65 (m, 2H, Ar-**H**), 7.30 (t, 1H, *J* = 6.9), 3.45 - 3.57 (4 Hs overlap in solvent peak, -NH**CH_2**$CH_2CH_2CH_2CH_2$ **CH_2**NH-), 1.37~2.02 (m, 8H, -$NHCH_2$**$CH_2CH_2CH_2CH_2$**CH_2NH-); ^{13}C-NMR (75 MHz, DMSO-d_6) δ 159.7, 150.2, 149.1, 138.7, 136.3, 135.9, 130.5, 130.4, 127.3, 126.5, 124.9, 121.6, 120.4, 117.3, 41.1 - 39.2 (2 Cs overlap in solvent peak.), 29.1, 28.9, 26.8, 26.6; HRESI-MS: calcd., 422.1815 $[M]^+$, 423.1893 $[M+H]^+$; found, 423.1931 $[M+H]^+$, 445.1720 $[M+Na]^+$.

3-(7-[(1-Oxido-1,2,4-benzotriazin-1-ium-3-yl)amino]heptylamino)-1,2,4-benzotriazine-1,4-dioxide (9f)

Red solid (45% yield); mp 202-204 °C; IR (KBr, cm^{-1}) 3334, 3206, 3109, 2928, 2855, 1578; ^{1}H-NMR (300 MHz, DMSO-d_6) δ 8.38 (s, 1H, Ar-**NH**-), 8.17 (d, 1H, *J* = 9, Ar-**H**), 8.09 - 8.11 (m, 2H, Ar-**H**), 7.88 - 7.94 (m, 2H, Ar-**H** and Ar-**NH**-), 7.72 (t, 1H, *J* = 6.9, Ar-**H**), 7.50-7.55 (m, 2H, Ar-**H**), 7.29 (t, 1H, *J* = 6, Ar-**H**), 3.45 - 3.57 (4 Hs overlap in solvent peak, -NH**CH_2**$CH_2CH_2CH_2$ CH_2CH_2-**CH_2**NH-), 1.34 - 1.58 (m, 10H, -$NHCH_2$**$CH_2CH_2CH_2$** **CH_2CH_2**CH_2NH-); ^{13}C-NMR (75 MHz, DMSO-d_6) δ 159.6, 150.4, 149.0, 138.7, 136.2, 135.9, 130.5, 130.4, 127.3, 126.5, 124.9, 121.6, 120.4, 117.3, 41.1 - 39.2 (2 Cs overlap in solvent peak.), 29.0, 28.8, 26.7, 26.5; HRESI-MS: calcd., 436.1971 $[M]^+$, 437.2050 $[M+H]^+$; found, 437.2075 $[M+H]^+$, 459.1893 $[M+Na]^+$.

3-(8-[(1-Oxido-1,2,4-benzotriazin-1-ium-3-yl)amino]octylamino)-1,2,4-benzotriazine-1,4-dioxide (9g)

Red solid (15% yield); mp 198-200 °C; IR (KBr, cm^{-1}) 3288, 3063, 2926, 2851, 2360, 1614, 1570; ^{1}H-NMR (300 MHz, DMSO-d_6) δ 8.39 (s, 1H, Ar-**NH**-), 8.18 (d, 1H, *J* = 8.7, Ar-**H**), 8.09 - 8.12 (m, 2H, Ar-**H**), 7.91 - 75 (m, 2H, Ar-**H** and Ar-**NH**-), 7.75 (t, 1H, *J* = 7.2, Ar-**H**), 7.53 - 7.55 (m, 2H, Ar-**H**), 7.31 (t, 1H, *J* = 7.5, Ar-**H**), 3.45 - 3.57 (4 Hs overlap in solvent peak, -NH**CH_2**CH_2CH_2 $CH_2CH_2CH_2CH_2$**CH_2**NH-), 1.22 - 1.57 (m, 12H, - $NHCH_2$**CH_2CH_2** **$CH_2CH_2CH_2CH_2$**CH_2NH-); ^{13}C-NMR (75 MHz, DMSO-d_6) δ 159.6, 150.4, 149.5, 138.7, 136.2, 136.0, 130.6, 130.4, 127.4, 126.6, 125.0, 121.6, 120.4, 117.4, 41.2 - 39.2 (2 Cs overlap in solvent peak.), 29.1 - 28.9 (4 Cs), 26.7, 26.5; HRESI-MS: calcd., 450.2128 $[M]^+$, 451.2206 $[M+H]^+$; found, 451.2230 $[M+H]^+$, 473.2055 $[M+Na]^+$.

Synthesis of Bis(3-amino-1-oxo-1,2,4-benzotriazinyl)-alkane (10)

Compound **3** (0.36g, 2.0 mmol) was dissolved in ethanol (7.5 mL) then added the respective diaminoalkanes reagent (1 mmol) and TEA (0.28 mL) and then heated to reflux over 6 hrs. The reaction was cooled to room temperature, followed by filtering and washing (30 mL) with water to afford yellow solid compounds **10a** and **10b**.

Bis(3-amino-1-oxido-1,2,4-benzotriazin-3-yl)-ethane (10a)

Yellow solid (quant.); mp: 231-233 °C (after recrystallization by hot methanol); IR (KBr) cm^{-1} 3381, 3338, 2935, 2343, 1570; ^{1}H-NMR (300 MHz, DMSO-d_6) δ 8.12 (d, 2H, *J* = 8.7 *Hz*, Ar-**H**), 7.94 (s, 2H, Ar-**NH**-), 7.75 (t, 2H, *J* = 8.1 Hz, Ar-**H**), 7.44 (d, 2H, *J* = 8.4 Hz, Ar-**H**), 7.33 (t, 2H, *J* = 8.4 HZ, Ar-**H**), 3.61 (s, 4H, -**CH_2 CH_2**-); ^{13}C-NMR (75 MHz, DMSO-d_6) δ 159.8, 148.9, 136.4, 130.8, 126.6, 125.3, 120.5, 41.2 - 39.3 (2 Cs overlap in solvent peak.); HRMS(EI) m/z: calcd., 350.3451 $[M]^+$; found, 350.1248 $[M]^+$.

Bis(3-amino-1-oxido-1,2,4-benzotriazin-3-yl)-propane (10b)

Yellow solid (quant.); mp: 224-226 °C (after recrystallization by hot methanol); IR (KBr) cm^{-1} 3291, 2928, 2861, 2363, 2325, 1585; ^{1}H-NMR (300 MHz, DMSO-d_6) δ 8.03 (d, 2H, *J* = 8.7 Hz, Ar-**H**), 7.90 (s, 2H, Ar-**NH**-), 7.68 (t, 2H, *J* = 7.5 Hz, Ar-**H**), 7.43 (d, 2H, *J* = 8.4 Hz, Ar-**H**), 7.25 (t, 2H, *J* = 7.5 Hz, Ar-**H**), 3.46 (s, 4H, -**$CH_2CH_2CH_2$**-), 1.90 (s, 2H, -CH_2**CH_2**CH_2-); ^{13}C-NMR (75 MHz, DMSO-d_6) δ 159.8, 149.0, 136.3, 130.7, 126.5, 125.0, 120.5, 38.6 (2 Cs), 28.5; HRMS(EI) m/z: calcd., 364.3722 $[M]^+$; found, 364.1412 $[M]^+$.

2.2. Physicochemical Measurements

The hydrophobicity of TPZ and TPZ derivatives **7** and **8** were determined by HPLC analysis of drug distribution between octanol and aqueous buffer phase at pH 7.4 as previously described [29, 30].

2.3. HPLC Conditions

The chromatographic analysis was performed on a Merck KGaA LiChroCART stainless steel Purospher STAR cartridges-RP-18E (4.6 mm x 150 mm, 5 μm) at a column temperature of 25 °C and flow rate of 0.5 mL/min at isocratic elution, respectively, and monitored at 285 nm, according to the UV absorption of the sample. All compounds were dissolved in DMSO or methanol. The mobile phase was composed of water : acetonitrile (70 : 30) including 0.7% acetic acid.

2.4. Cell Culture

Human breast cancer cell line (MCF-7, BCRC 60436), human colon cancer cell line (HCT-116, BCRC 60349) and human non-small cell lung cancer cell line (NCI-H460, BCRC 60373) were purchased from Bioresource Collection and Research Center (BCRC), Food Industry Research and Development Institute (FIRDI, Hsinchu City, Taiwan). MCF-7 and HCT-116 cells were cultured in Dulbecco's Modified Eagle's Medium (Gibco, Grand Island, New York, USA) with 10% fetal bovine serum (Gibco, Grand Island, New York, USA), sodium pyruvate (Sigma, St. Louis, Missouri, USA), and 1.5 g/L sodium bicarbonate (Sigma, St. Louis, Missouri, USA) at 37 °C in a humidified atmosphere at 5% CO_2. NCI-H460 cells were cultured in RPMI 1640 medium with 10% fetal bovine serum (Gibco, Grand Island, New York, USA), sodium pyruvate (Sigma, St. Louis, Missouri, USA), 1.5 g/L sodium bicarbonate (Sigma, St. Louis, Missouri, USA) and 10 mM HEPES (Sigma, St. Louis, Missouri, USA).

2.5. Biological Assays

The efficacy of the TPZ derivatives in killing aerobic and hypoxic MCF-7, HCT-116 and NCI-H460 *in vitro* after drug exposure under different conditions over 24 hours was determined by MTT assay at 545 nm. In general, cells were cultured in 96-well plates (20000 cells / well) in culture medium with normoxic condition (20% O_2, 5% CO_2 at 37 °C). After 24 hours, compounds spanned at different concentrations were added and treated to cell cultures for another 24 hours in normoxic condition. In hypoxic cytotoxicity assay, cells were treated serial concentrations and hypoxic condition (3% O_2 at 37 °C). After 6 hours, the tested cell cultures were moved to normoxic condition and culturing was continuing for another 18 hours. Survival cells were determined as concentration-dependent to inhibit cell proliferation to 50% of control (IC_{50}), and the ratio of cytotoxicity between hypoxia and normoxia for TPZ derivatives was calculated as the hypoxic cytotoxicity ratio [HCR; IC_{50} (normoxia)/IC_{50} (hypoxia)]. For each experiment, TPZ was included as a positive control.

2.6. Cell Cycle Assay by Flow Cytometry

After each compound was exposed to both hypoxia and normoxia, HCT-116 cells were harvested and washed with PBS. Then the cells were centrifuged (350 g, 5 min) and fixed with 75% ethanol at -20 °C for overnight. The fixed cells were centrifuged and supernatant was removed. The cells were re-suspended in 1 ml of PBS containing 100 μg/ml RNase, 1% triton X-100, propidium iodide (20 μg/ml) and incubated at 37 °C in the dark for 30 mins. After incubation, stained cells were analyzed by FACSCalibur flow cytometer (BD Biosciences).

2.7. ROS Analysis by Flow Cytometry

The ROS determination was according to the manufacturer's protocols with a little modification. ROS level was measured by CM-H_2DCFDA (5-(and-6)-chloromethyl-2',7'-dichlorodihydro-fluorescein diacetate, acetyl ester), an oxidative stress indicator, Invitrogen). HCT-116 cells were treated with/without TPZ and **9a** for 24 hours. Cells were stained by CM-H_2DCFDA for 45 minutes. Cells were collected and ROS levels were detected by FACSCalibur flow cytometer (BD Biosciences).

2.8. Fluorescent Inhibitor of Caspase Activity (FLICA) by Flow Cytometry

Level of caspase 3/7 after treatment with compounds was determined by FLICA assay. Experiments were conducted by FAM-FLICA^{TM} kit according to the manufacturer's protocols. Briefly, HCT-116 cells were harvested and washed with PBS after compounds respectively treated in hypoxia or normoxia for 24 hrs. Then the cells were centrifuged (350 g, 5 minutes) and stained by FAM-FLICA^{TM} kit. After staining, the cells were analyzed by flow cytometer (BD Biosciences).

2.9. Assay of Level of γ-H2AX and Cleaved PARP by Flow Cytometry

HCT-116 cells were incubated with serial concentrations of TPZ and **9a** for 24 hours in normoxia and hypoxia, respectively. After treatment, cells were harvested by centrifuged for 5 minutes at 300 g and fixed by BD Cytofix/Cytoperm fixation/permeabilization solution. After fixation, cells were stained by Alexa Fluor® 647 conjugated mouse anti-H2AX (pS139) (BD Pharmingen™) and PE conjugated mouse anti-cleaved PARP (BD Pharmingen™) according to the manufacturer's protocols. Briefly, cells were incubated with antibodies for 20 minutes at room temperature and subsequently analyzed by flow cytometry (BD Biosciences).

2.10. *In vitro* Tube Formation Test

Experiments on *in vitro* tube formation were conducted in quadruplicate in 24-well plates using angiogenesis kit (Kurabo, Japan) according to the manufacturer's protocols. Briefly, HUVECs

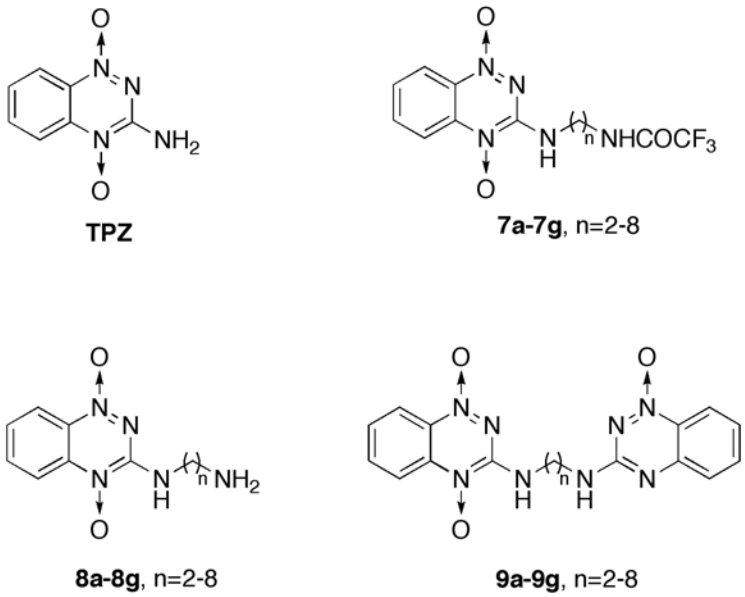

Fig. (1). General structures of tirapazamine (TPZ) and TPZ derivatives.

and fibroblasts were co-cultured in 24-well plates with basal medium or solvent control medium (basal medium containing 0.2% DMSO) or solvent control medium containing TPZ, **7b**, **8g, 9a** and **9b** (2 and 20 μM), respectively. The medium renewal with or without the tested compound in cultures was conducted every 3 days. Co-cultured HUVECs with fibroblasts were performed for a total of 11 days. HUVECs was then stained with anti-CD31 antibody according to the manufacturer's protocols. The tube formation tube area, lengths, and joints were measured quantitatively over 5 different fields for each condition using an image analyzer (Kurabo).

2.11. Statistical Analysis

Dose-response relationships were constructed by linear regression of the percent inhibition of parameters derived in the preceding sections against log drug concentrations. Each value was expressed as the mean ± SEM. IC_{50} values were calculated from the regression lines. The statistical significance of difference was assessed with one-way analysis of variance (ANOVA) followed by Tukey's post hoc analysis using GraphPad Prism 6 to determine statistical significance as *p* values of less than 0.05.

3. RESULTS AND DISCUSSION

3.1. Chemistry

The reasonable efficiency of the 3-amino-1,2,4-benzotriazine-1,4-dioxide (tirapazamine, TPZ) synthesis has been previously established [31]. In this work, structural modifications were made using extended-alkyl linkers without or with an extra heterocyclic moiety at 3-NH_2 on the B-ring of TPZ to afford 3-amino-1,2,4-benzotriazine-1,4-dioxide bearing either alkyl linkers only (compounds **7** and **8**) or alkyl linkers extended with 3-amino-1,2,4-benzotriazine-1-oxide moiety (compound **9**) (Fig. **1**).

During the synthesis of TPZ derivatives, a key intermediate **3**, in 75% yield, was generated, as described elsewhere [32] (Scheme **1**). Unfortunately, intermediate **3** failed to be converted to compound **11 (**3-chloro-1,2,4-benzotriazine-1,4-dioxide), which is an alternative key precursor in the preparation of TPZ derivatives, and it was superseded by recovering quantitative intermediate **2**. Therefore, TPZ derivatives **7**, **8** and **9** were synthesized according to Schemes **2** and **3** using a modified version of previously described procedures [10, 33].

Briefly, dioxide compound **7** were formed with yields of 29 - 50 %, along with the corresponding precursor of compound **6** (20 - 40% recovery), by the oxidation of 3-amino-1,2,4-benzotriazine-1-oxide that bore alkyl-trifluoroacetamides (compounds **6**), using trifluoroperacetic acid ($H_2O_2/(CF_3CO)_2O$). Compound **6** were formed in a substitution reaction with intermediate **3** coupled with the corresponding alkyl-trifluoroacetamides (compound **5**) that had been previously prepared and purified by chromatography from the corresponding homologue-alkyl diamine with trifluoroacetic anhydride. Compound **6** was also oxidized by *m*CPBA to yield compounds **7**, but the yields were poor. Further de-protection of the trifluoroacetamido group with ammonium hydroxide caused compound **7** to be converted into the counterpart primary amine compound **8** in quantitative (~ 99%) yield.

To obtain a high yield of compound **9**, synthetic approaches that can be found in early studies in the field [16, 23] were modified as in Scheme **2**. A straightening reaction of compound **8** with an intermediate **3** formed 3-amino-1,2,4-benzotriazine-1,4-dioxide bearing the counterpart alkyl linkers that were extended with an 3-amino-1,2,4-benzotriazine-1-oxide (compound **9**), in 14 - 45 % yields. Even though chloride **3** was successfully coupled with the alkyl-amino groups of **8a**, **8b** and **8d**, forming the corresponding **9a** (35%), **9b** (17%) and **9d** (14%), respectively, when refluxed in methanol, chloride **3** did not couple with **8e**, **8f** and **8g** in the same manner, and equal volumes of methanol and propanol were used instead of methanol only, the counterpart reaction, to yield the corresponding **9e** (37%), **9f** (45%) and **9g** (15%), respectively.

An alternative synthesis of compound **9,** Scheme **3,** was carried out, in which diaminoalkanes **4a** and **4b** reacted with chloride **3** to give the corresponding compounds **10a** and **10b** in approximately 80% yield; these products were then oxidized with trifluoroperacetic acid ($H_2O_2/(CF_3CO)_2O$) under acidic conditions to yield trace amounts (5% yield) of compounds **9a** and **9b**, along with many unidentified side products. Unfortunately, almost 20-30% of **10a** and **10b** were recovered.

In this work compound **9**, except for **9a** and **9b**, exhibited poor solubility owing to their relatively longer homologue-alkyl linker with di-heterocyclic benzotriazine, supposed to make subsequent bioassays difficult.

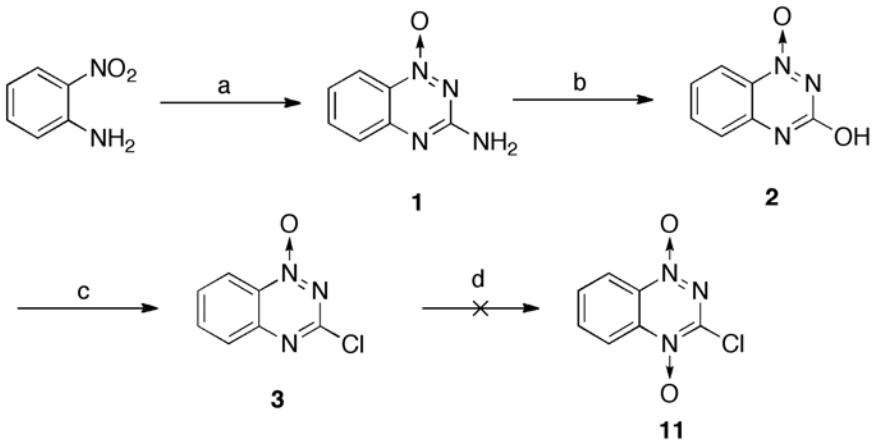

Scheme 1. Synthesis of key TPZ intermediates. *Reagents and Conditions*: (**a**) (i) $NCNH_2$, 80 °C (ii) 37% HCl, 100 °C, then NaOH, 100 °C; (**b**) (i) conc. H_2SO_4, 0 °C (ii) $NaNO_2$, RT; (**c**) $POCl_3$, reflux; (**d**) trifluoroperacetic acid (H_2O_2/$(CF_3CO)_2O$), DCM, RT

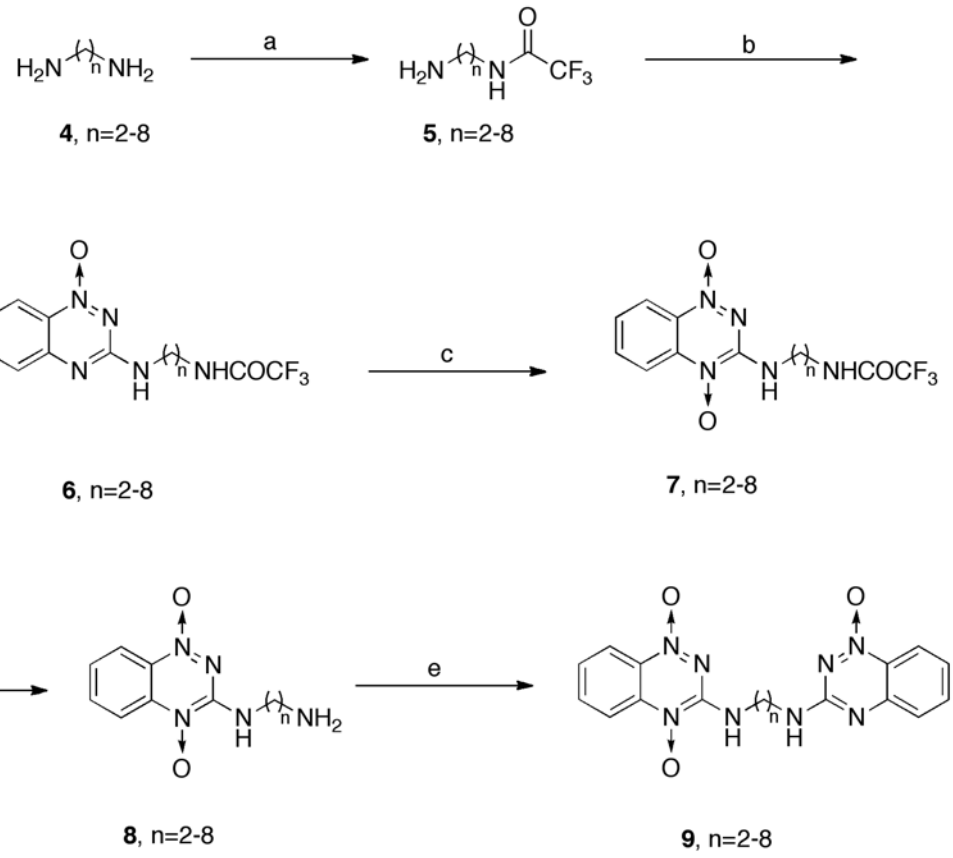

Scheme 2. Synthesis of key TPZ derivatives. *Reagents and Conditions*: (**a**) TFAA, TEA, DCM, -20 °C; (**b**) **3**, TEA, EtOH, reflux; (**c**) (i) TFA, DCM, 0 °C (ii) trifluoroperacetic acid (H_2O_2/$(CF_3CO)_2O$), RT; (**d**) NH_4OH, MeOH, RT; (**e**) **3**, TEA, MeOH or MeOH/1-propanol (1:1), reflux.

3.2. Biologicals

3.2.1. Differential in vitro Cytotoxicity between Normoxia and Hypoxia

Twenty-one TPZ derivatives, including known compounds such as **7c**, **7d**, **7e**, **8b**, **8c**, and **8d** [16, 27, 28], were synthesized to evaluate their *in vitro* cytotoxicity in MCF-7, HCT-116 and NCI-H460 cells between normoxia and hypoxia, by MTT assay (Table **1**). TPZ was used as a positive control.

Systematically screening synthesized TPZ derivatives for cytotoxicity revealed that all compounds **7** (with IC_{50}s of about 29 - 46 μM, and potencies that were 1.79 - 1.13 times that of TPZ) were more cytotoxic than TPZ (IC_{50} = 52 μM) in hypoxia and **7a-7g** exhibited considerably less normoxic toxicity in MCF-7 cells. Generally, **7a-7g** had more potent hypoxic cytotoxicity than normoxia in both NCI-H460 and HCT-116 (Table **1**). Clearly, of compounds **7**, compound **7a** exhibited higher hypoxic cytotoxicity than TPZ in MCF-7, NCI-H460 and HCT-116 cells (Table **1**).

Generally, compound **8** were less toxic toward MCF-7, NCI-H460 and HCT-116 cells than compound **7** in both normoxia and hypoxia with the exception that **8a** was comparable to compound **7** toward MCF-7 (IC_{50} at normoxic 68.0 μM, and hypoxic 33.4 μM),

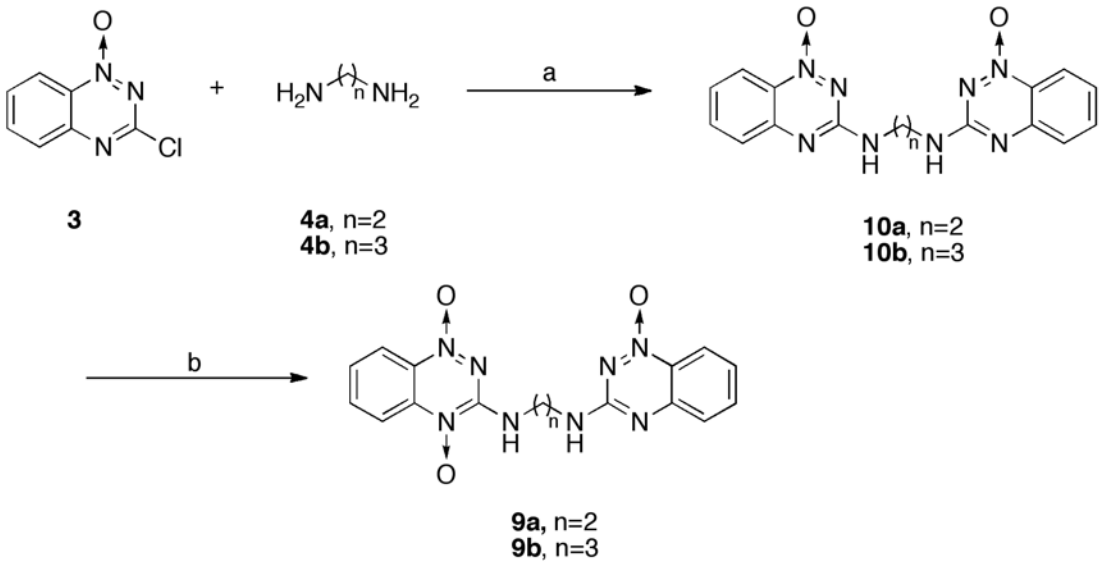

Scheme 3. Alternative synthesis of key TPZ derivatives. *Reagents and Conditions*: (a) EtOH, reflux; (b) TFA, DCM, trifluoroperacetic acid, RT.

NCI-H460 (IC_{50} at normoxic 18.7 μM, and hypoxic 10.1 μM) and HCT-116 (IC_{50} at normoxic 40.3 μM and hypoxic 22.4 μM) cells.

Compounds **9a** and **9b** generally had a greater effect on MCF-7 (corresponding IC_{50} at normoxic > 70 and 68.3 μM, respectively, and at hypoxic 11.7 and 24.0 μM, respectively), on NCI-H460 (corresponding IC_{50} at normoxic 43.7 and 44.6 μM, respectively, and at hypoxic 17.5 and 21.4 μM, respectively) and on HCT-116 cells (corresponding IC_{50} at normoxic 66.3 and 53.8 μM, respectively, and at hypoxic 18.1 and 28.7 μM, respectively). These results showed that compounds **9a** and **9b** were more potent than TPZ (for MCF-7 cells with IC_{50} at normoxic 326.5 μM and hypoxic 52.1 μM; for NCI-H460 cells with IC_{50} at normoxic 85.0 μM and hypoxic 32.9 μM; and for HCT-116 cells with IC_{50} at normoxic 89.1 μM and hypoxic 34.8 μM), especially under hypoxia.

For all synthesized TPZ derivatives, the corresponding hypoxic cell selectivity [HCR = IC_{50} (aerobic)/IC_{50} (hypoxia)] spanned approximately a 5.0-fold range from 1.3 to 6.3 in MCF-7, a 2.4-fold range from 1.2 to 2.6 in NCI-H460 and a 2.4-fold range from 1.3 to 3.7 in HCT-116 (Table **1**).

In MCF-7 cells, most of the TPZ derivatives in this study exhibited moderate hypoxic selectivity (HCR = 1.3 - 3), but **7b** (HCR = 5.7) and **9a** (HCR > 6.0) exhibited greater hypoxic selectivity, comparable to that of TPZ (HCR = 6.3). In NCI-H460, most of the TPZ derivatives exhibited less than significant hypoxic selectivity (1.2 - 1.8). However, compound **7b** (HCR = 2.6), **9a** (HCR = 2.5) and **9b** (HCR = 2.1) had greater hypoxic selectivity similar to that of TPZ (HCR = 2.6). In HCT116, most of the TPZ derivatives exhibited modest hypoxic selectivity (HCR = 1.3 - 1.9), but **7d** (HCR = 2.2), **7f** (HCR = 2.1), **7g** (HCR = 2.2) and **8g** (HCR = 2.2) had a similar hypoxic selectivity to TPZ (HCR = 2.6). Compound **9a** (HCR = 3.7) exhibited greater hypoxic selectivity than TPZ.

Compound **7** generally exhibited greater potency than compound **8** (derived from the corresponding compounds **7**), suggesting that the trifluoroacetamide moiety, as an electron-withdrawing group at the ultimate position of the 3-alkyl side chain of 3-amino-1,2,4-benzotriazine-1,4-dioxide (TPZ), enhanced hypoxic cytotoxicity toward the three cancer cell lines (NCI-H460, HCT-116, and MCF-7) in this work. Among the synthesized TPZ derivatives, **9a** and **9b** were most potent under hypoxic conditions for the three cancer cell lines. The extraordinary presence of an extra 1,2,4-benzotriazine-1-oxide chromophore in a basic 3-side chain of compounds **9**, including **9a** and **9b**, enhanced hypoxic cytotoxicity, but unfortunately most of the compound **9** had limited IC_{50}s owing to poor solubility, which caused the compound to be precipitated at concentrations of greater than 30 μM.

3.2.2. Log P

To determine whether hydrophobicity/hydrophilicity affects the hypoxic cell cytotoxicity of synthesized TPZ derivatives, the partition coefficients (log P) of compounds **7** and **8** were systematically measured at physiological pH. The distributions of TPZ and TPZ derivatives between octanol and phosphate buffer solution (pH = 7.4) were determined at the corresponding retention time of compounds **7** and **8** by HPLC analysis (Table **2** and Fig. **2**).

Generally, a longer alkyl side chain in compounds **7** or **8** corresponded to a higher log P value. All of compound **8** (with log $P_{7.4}$ < -0.85 to -2.4) had a lower log P than TPZ (-0.4 in this study, -0.32 to - 0.34 in pervious report [29]) and compounds **7** had a log $P_{7.4}$ of greater than 0.52 to 2.4. Polar side chains such as either primary alkylamines (compounds **8**) or nonpolar trifluoroacetamido-alkyl moieties (compounds **7**) at the 3-position of TPZ might have influenced the solubility of those TPZ derivatives in water. This characteristic of compounds **7** and **8** between hydrophobicity and hypoxic cytotoxicity in HCT-116 yielded a general reverse parabolic curve. The optimal hypoxic cytotoxicity of compound **7** was correlated with log P ranged from zero to one and that of compound **8** was correlated with log P from negative unity to zero. Compound **8a** was an outlier on the curve. This relationship suggests that optimal lipophilicity/hydrophilicity may be important in the structure-activity of compounds **7** and **8**.

Clearly, when the alkylamines (such as compound **8,** but not compound **8a**) or lipophilic trifluoroacetamidoalkyl moiety (as in compounds **7**, but not **7a**) that was into the 3-position of 1,2,4-benzotriazine-1,4-dioxide was more hydrophilic, but the cytotoxicity and selectivity were lower. However, the hypoxic cytotoxicity and selectivity of TPZ derivatives such as **9a** and **9b** increased when a 1,2,4-benzotriazine-1-oxide chromophore, rather than an amine or trifluoroacetamide group was introduced.

The above results are consistent with evidence that extended aromatic or alkyl groups at the 3-position of 1,2,4-benzotriazine-1,4-dioxide increase lipophilicity, hypoxic cytotoxicity and HCR [16, 23, 34]. Although some studies have demonstrated that TPZ

Table 1. Cytotoxicity of TPZ derivatives against MCF-7, NCI-460, and HCT-116 cancer cells in both normoxia and hypoxia.

Comp'd	R_1	R_2	Cytotoxicity (IC_{50}, μM)					
			MCF-7[d]		NCI-H460[d]		HCT-116[d]	
			N[a]	H[b]	N[a]	H[b]	N[a]	H[b]
TPZ	H	-	326.5±10.8	52.1±7.9	85.0±9.7	32.9±2.1	89.1±14.5	34.8±8.3
7a	$(CH_2)_2NHCOCF_3$		50.0±5.2	29.0±14.0	44.2±5.0	17.2±4.0	44.0±17.2 **	33.8±13.1
7b	$(CH_2)_3NHCOCF_3$	-	165.1±10.2	29.1±13.5	89.8±9.8	55.9±7.4	55.4±4.7 *	38.6±8.1
7c	$(CH_2)_4NHCOCF_3$	-	> 116	35.7±7.9	ND	ND	ND	ND
7d	$(CH_2)_5NHCOCF_3$	-	> 111	39.9±10.5	70.8±27.3	43.0±12.6	65.4±14.6	44.1±10.2
7e	$(CH_2)_6NHCOCF_3$	-	> 107	46.7±1.0	ND	ND	110.0±2.2	63.9±3.8
7f	$(CH_2)_7NHCOCF_3$	-	> 103	42.2±0.3	88.7±26.4	46.8±20.3	105.8±2.0	47.9±3.7
7g	$(CH_2)_8NHCOCF_3$	-	60.6±6.2	32.8±6.4	91.0±50.9	46.0±24.1	108.0±21.3	50.5±7.1
8a	$(CH_2)_2NH_2$	-	68.0±2.2	33.4±9.4	18.7±2.7	10.1±3.7	40.3±14.6 ***	22.4±9.7
8b	$(CH_2)_3NH_2$	-	170.2±4.0	65.8±2.4	95.6±33.9	79.5±26.6	90.4±3.5	54.8±8.0**
8c	$(CH_2)_4NH_2$	-	156.0±4.1	112.3±11.4	120.5±28.2	75.6±24.0	100.0±10.4	64.0±12.5***
8d	$(CH_2)_5NH_2$	-	> 76	> 76	101.0±38.9	83.4±33.8	93.7±20.0	55.3±7.5*
8e	$(CH_2)_6NH_2$	-	150.2±26.0	110.1±9.4	104.4±15.1	68.7±15.1	91.2±16.2	62.9±11.0***
8f	$(CH_2)_7NH_2$	-	> 90	88.6±0.1	79.4±22.6	42.8±8.3	78.3±4.9	40.8±4.3
8g	$(CH_2)_8NH_2$	-	213.9±26.0	74.3±21.1	82.7±20.4	45.8±6.1	97.0±8.7	44.8±6.0
9a	$(CH_2)_2$	3-amino-1,2,4- benzotriazine-1-oxide	> 70	11.7±0.9	43.7±12.5	17.5±4.3	66.3±16.5	18.1±2.6*
9b	$(CH_2)_3$	3-amino-1,2,4- benzotriazine-1-oxide	68.3	24.0±3.3	44.6±4.3	21.4±4.8	53.8±4.7**	28.7±6.7
9c	$(CH_2)_4$	3-amino-1,2,4- benzotriazine-1-oxide	> 30[c]	> 30[c]	> 30[c]	> 30[c]	> 30[c]	> 30[c]
9d	$(CH_2)_5$	3-amino-1,2,4- benzotriazine-1-oxide	> 30[c]	> 30[c]	> 30[c]	> 30[c]	> 30[c]	> 30[c]
9e	$(CH_2)_6$	3-amino-1,2,4- benzotriazine-1-oxide	> 30[c]	> 30[c]	> 30[c]	> 30[c]	> 30[c]	> 30[c]
9f	$(CH_2)_7$	3-amino-1,2,4- benzotriazine-1-oxide	> 30[c]	> 30[c]	> 30[c]	> 30[c]	> 30[c]	> 30[c]
9g	$(CH_2)_8$	3-amino-1,2,4- benzotriazine-1-oxide	> 30[c]	> 30[c]	> 30[c]	> 30[c]	> 30[c]	> 30[c]

[a]N = normoxia: the percentage of oxygen is 20%.; [b]H = hypoxia: the percentage of oxygen is 3%; [c]limited IC_{50}s due to poor solubility which compounds were precipitated when concentration is greater than 30 μM; [d] hypoxiaic cytotoxicity ratio, HCR = IC_{50} (aerobic)/IC_{50} (hypoxia). Data was shown as Mean ± SEM, n=3. Differences were considered statistically significant on the basis of TPZ as *, $p<0.01$; **, $p<0.005$; ***, $p<0.001$.

passes into cells by passive diffusion in a concentration-dependent manner [15, 32], this work indicates the optimal lipophilicity of TPZ derivatives compounds **7** and **8** in relation to the corresponding hypoxic cytotoxicity as well.

3.2.3. Mechanism Studies (Cell Cycle, ROS, Caspase Activity, and Apoptosis Assays using Flow Cytometry)

To examine the modes of action of the synthesized TPZ derivatives, the effects of the compounds **9a** and **9b** on the cell cycle of HCT-116 cells were studied using flow cytometry with propidium iodide (PI) stain. The HCT-116 cells were initially treated with **9a**, **9b** and TPZ at 15 or 30 μM for 24 hours in normoxia and hypoxia, respectively, and the cell cycle profiles were determined (Table **3** and Fig. **3**).

First, in normoxia, the sub-G1 level of HCT-116 cells that were exposed to the tested compounds (TPZ, **9a** and **9b**, respectively) at 15 μM, was approximately 2.6%, 2.7% and 2.8% which did not differ significantly from that of the solvent control (~ 3%), whereas in hypoxia, HCT-116 cells following treatment with TPZ, **9a** and **9b** at 15 μM, respectively, the corresponding sub-G1 level was 7.3%, 13.1% and 4.3 (2.7% on control medium) (data of **9b** at 15 μM are not shown in Table **3** and Fig. **3**.). The results displayed that increasing effect on sub-G1 level of HCT-116 cells after treatment with **9a** at 30 μM was much greater than TPZ and **9b**. Therefore, we focused on **9a** at concentrations of 15 and 30 μM and **9b** at 30 μM, in comparison to TPZ, for elucidating mechanism studies. The cells that were exposed to 30 μM **9a** was slightly higher (3.8%) and for of the cells that were exposed to 30 μM **9a** was lower (2.1%) by **9b** at 30 μM, respectively. The corresponding G1 phase of HCT-116 cells in normoxia after treatment with TPZ, **9a** and **9b**, decreased in a concentration-dependent manner. Treatment with **9a** at 30 μM yielded a sub-G1 level of 24.3% level whereas treatment with the solvent control yielded a level of 54.3%; treatment with TPZ at 30 μM yielded a level of 35.3% and treatment with **9b** at 30 μM yield a level of 35.0%. No test compounds except for TPZ had an obvious effect on the S phase of the HCT-116 cells in normoxia. Interestingly, however, treatment with TPZ caused the accumulation of the HCT-116 cells in the G2/M phase (33.1% at 15 μM and 39.1% at 30 μM *vs.* 24.0% for the solvent control). Treatment with **9a** greatly arrested the G2/M phase (51.0% at 15 μM and 58.3% at 30 μM), whereas treatment with **9b** increased the G2/M phase (48.0% at 30 μM).

In hypoxia, the corresponding sub-G1 population after the treatment of HCT-116 cells with 15 μM TPZ or **9a** was 7.3% and 13.1%, the values of which should be compared with that following treatment with the solvent control (2.7%). Following treatment of HCT-116 cells in hypoxia with TPZ and TPZ derivatives (**9a** and **9b**) at 30 μM, the levels of the sub-G1 phase that were formed by TPZ, **9a** and **9b** were 16.5%, 24.3% and 12.2%, respectively. The corresponding G1 phase of the HCT-116 cells in hypoxia after treatment with TPZ, **9a** and **9b** was about half of that following treatment with the solvent control (60.0%). The tested compounds had no significant effect on the S phase of HCT-116 cells by those tested compounds in hypoxia.

Table 2. Partition coefficient, retention time, and cytotoxicity of TPZ derivatives (compounds 7 and 8), and their hypoxic cytotoxicity ratio against HCT-116 cell line.

	Log $P_{7.4}$[a]	Cytotoxicity (IC_{50}, μM)[b]	Retention time (minutes)	HCR[c]
TPZ	-0.42	34.8	4.41	2.6
7a	0.52	33.8	7.35	1.3
7b	0.63	38.6	8.49	1.4
7d	1.18	44.1	14.31	2.2
7e	1.77	63.9	22.52	1.7
7f	2.24	47.5	37.99	2.1
7g	2.40	50.5	69.06	1.3
8a	-2.15	22.4	2.55	1.8
8b	-1.98	54.8	2.93	1.7
8d	-2.01	55.3	3.70	1.7
8e	-1.52	62.1	4.36	1.5
8f	-1.14	40.8	4.49	1.9
8g	-0.81	44.8	5.59	2.2

[a]Log $P_{7.4}$ = log ($[solute]_{octanol}/[solute]_{water}$) at pH 7.4. [b]$IC_{50}$ = concentration of compounds for cell kill under hypoxia. [c]HCR = hypoxic cytotoxicity ratio IC_{50} (aerobic)/IC_{50} (hypoxic). All data were expression as Mean.

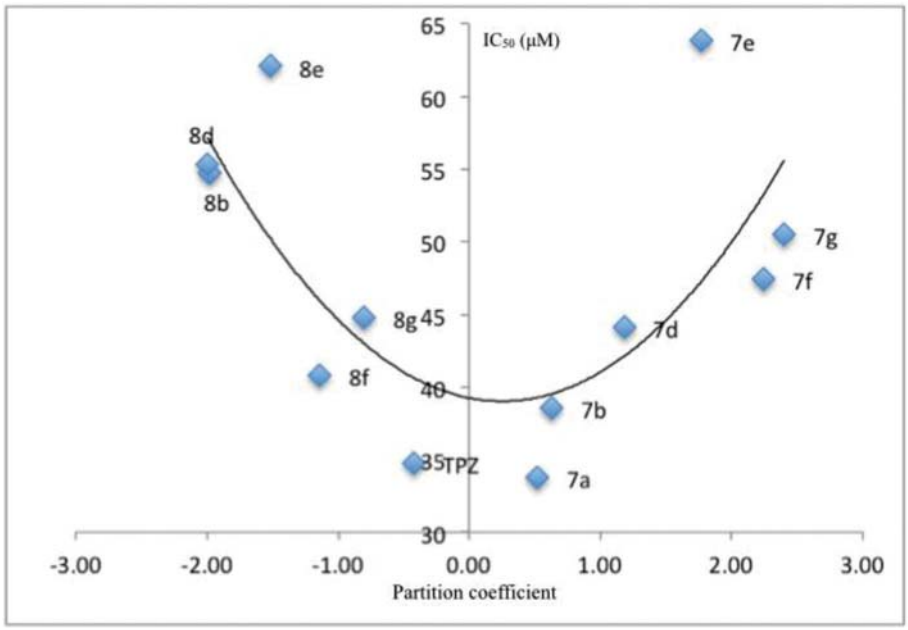

Fig. (2). The correlation between hypoxic cytotoxicity of tirapazamine derivatives (compounds **7** and **8**), and the corresponding partition coefficient values.

TPZ, **9a** and **9b** induced significantly increased the level of G2/M in HCT-116 cells in hypoxia, as displayed in Fig. **3** and Table **3**. The level of the G2/M phase in the HCT-116 cell cycle was three times higher than solvent control, except following treatment with **9a** at 30 μM**,** which around doubled the level only. The results concerning the cell cycle of HCT-116 following treatment with **9a**, **9b** or TPZ in normoxia revealed strong G2/M arrest, seemingly in response to loss of microtubule function.

Compound **9a** (58.3% G2/M accumulation level at 30 μM) had the strongest effect, but 1,2,4-benzotriazine-1-oxide (**1**), a key synthetic intermediate structurally related to **9a**, to treat HCT-116 cells (data not shown) was invalid. In hypoxia, **9a**, **9b** and TPZ caused G2/M cell cycle arrest of HCT-116, but interestingly **9a** caused less G2/M arrest (16.7% G2/M level at 30 μM) than did TPZ (27.3% at 30 μM). Low concentration (15 μM) of TPZ and **9a** more effectively induced for induction G2/M arrest (35.2% and 31.4% respectively) than did high concentration (30 μM), and this difference was especially evident for **9a**. In contrast, **9a**, **9b** and TPZ had the sub-G1 effect on the cell cycle in relation to the induction of apoptosis, of which **9a** had the strongest effect (24.3% at 30 μM).

Since TPZ can be metabolized to activated radicals and increase intracellular ROS, inducing DNA damage and apoptosis basically [11, 35, 36], whether compound **9a** induced an increase in ROS in HCT-116 cells, compared to TPZ, was determined by CM-H_2DCFDA (Invitrogen) using flow cytometry, according to the manufacturer's protocols. As presented in Fig. **4**, TPZ increased ROS by of 1.5- and 2-fold at 15 and 30 μM, relative to that of the control medium in normoxia, but increased ROS by factors of 6 and 10.5 at 15 and 30 μM, respectively, in hypoxia. HCT-116 cells that were exposed to **9a** at 15 and 30 μM exhibited 3.4- and 5.8-fold increase of ROS, respectively, in normoxia, but 46-and 60-fold

Table 3. Cell cycle profile of HCT-116 cells after treatment with TPZ and TPZ derivatives over 24 hours in both normoxia and hypoxia. Data were expression as Mean ± SEM, n=3.

		TPZ	9a	TPZ	9a	9b
In Normoxia	**Control**	**(15 μM)**	**(15 μM)**	**(30 μM)**	**(30 μM)**	**(30 μM)**
Sub-G1 (%)	3.0±1.5	2.6±2.2	2.7±0.7	3.2±0.5	3.8±1.7	2.1±0.1
G1 (%)	54.3±8.7	41.9±1.7	30.9±2.3	35.3±1.4	24.3±4.1	35.0±5.1
S (%)	18.1±5.1	21.9±2.4	15.0±5.5	22.1±2.9	12.9±5.2	14.3±4.1
G2/M (%)	24.0±3.3	33.1±3.7	51.0±4.2	39.1±4.0	58.3±2.8	48.0±1.9

		TPZ	9a	TPZ	9a	9b
In Hypoxia	**Control**	**(15 μM)**	**(15 μM)**	**(30 μM)**	**(30 μM)**	**(30 μM)**
Sub-G1 (%)	2.7±1.5	7.3±2.7	13.1±1.7	16.5±1.2	24.3±2.8	12.2±2.8
G1 (%)	60.0±8.0	22.5±9.4	26.2±3.7	26.3±5.5	33.3±2.4	28.1±1.2
S (%)	27.3±9.7	34.7±6.0	27.3±4.4	29.6±4.7	25.8±3.8	29.3±4.7
G2/M (%)	9.1±3.9	35.2±4.9	31.4±3.2	27.3±1.3	16.7±2.5	30.2±3.9

A

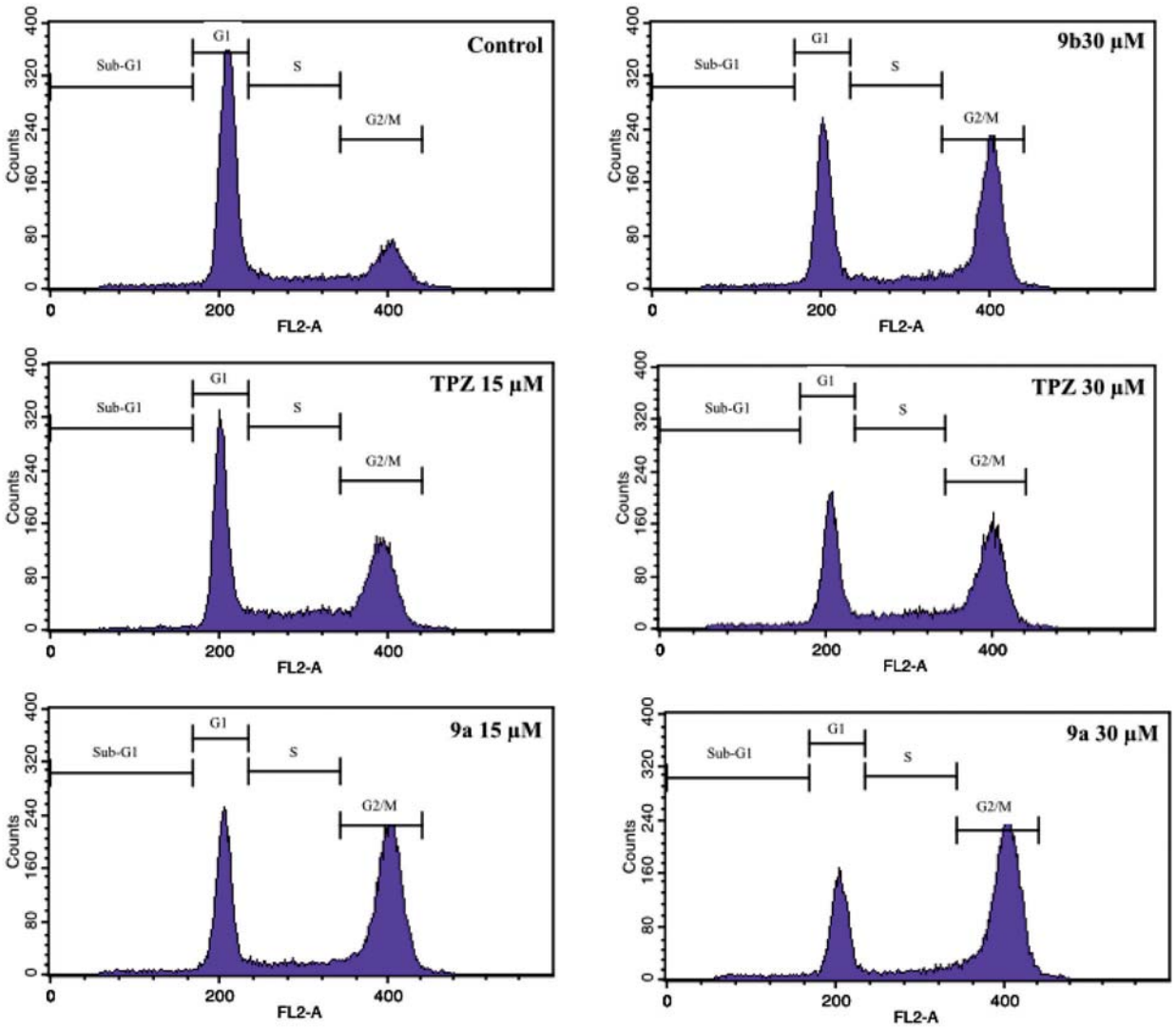

Fig. (3). contd….

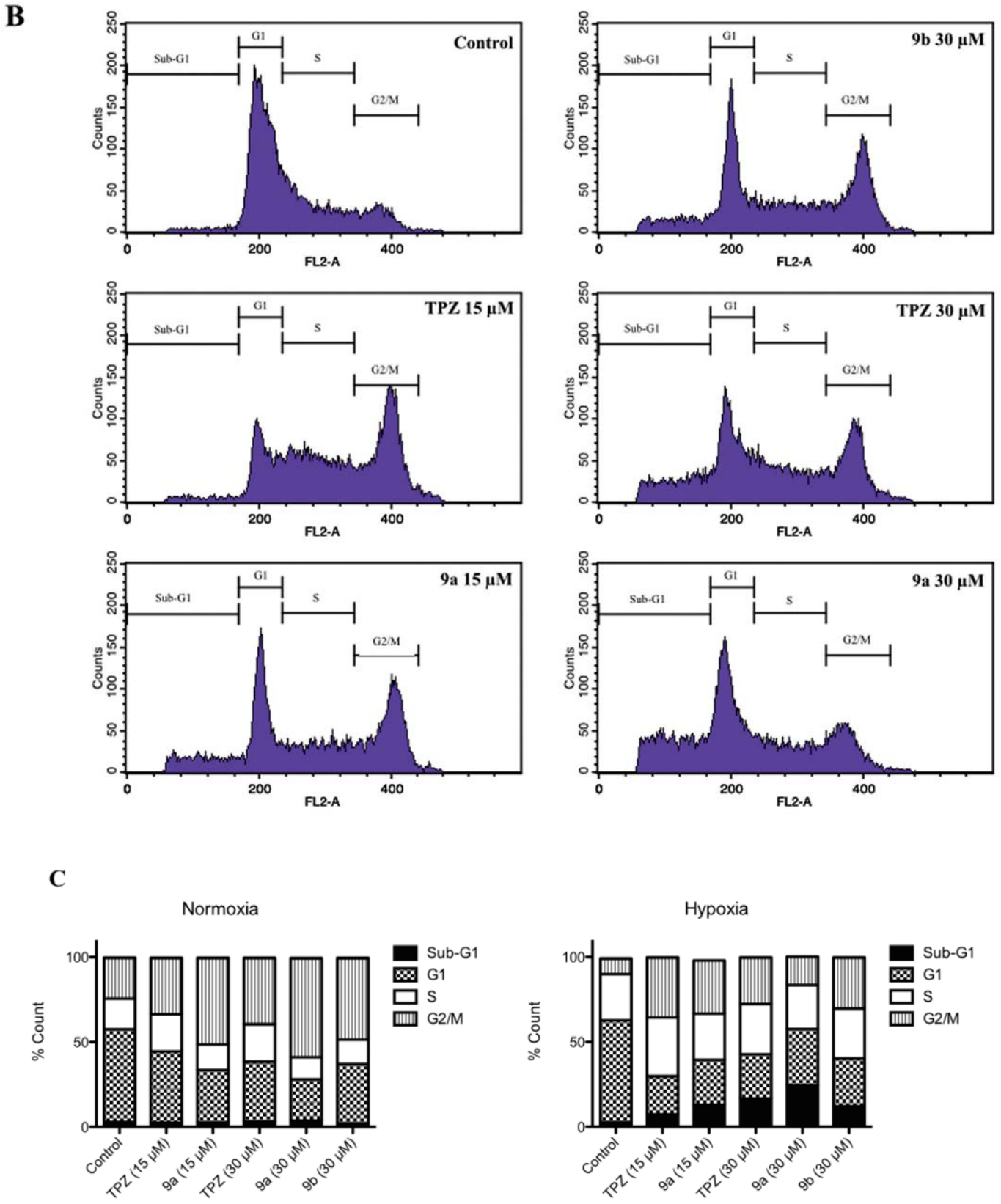

Fig. (3). TPZ derivatives increased cell apoptosis in hypoxia and influenced cell cycle profile compared to TPZ in HCT-116 cells. HCT-116 cells were treated with different concentrations of TPZ, **9a** and **9b** in both (A) normoxia or (B) hypoxia. After 24 hours, cells were stained by PI and apoptosis and cell cycle profile were detected by flow cytometry. (C) The effects of TPZ, **9a** and **9b** in cell cycle profile in both normoxia and hypoxia. Data were expressed as Mean, n=3.

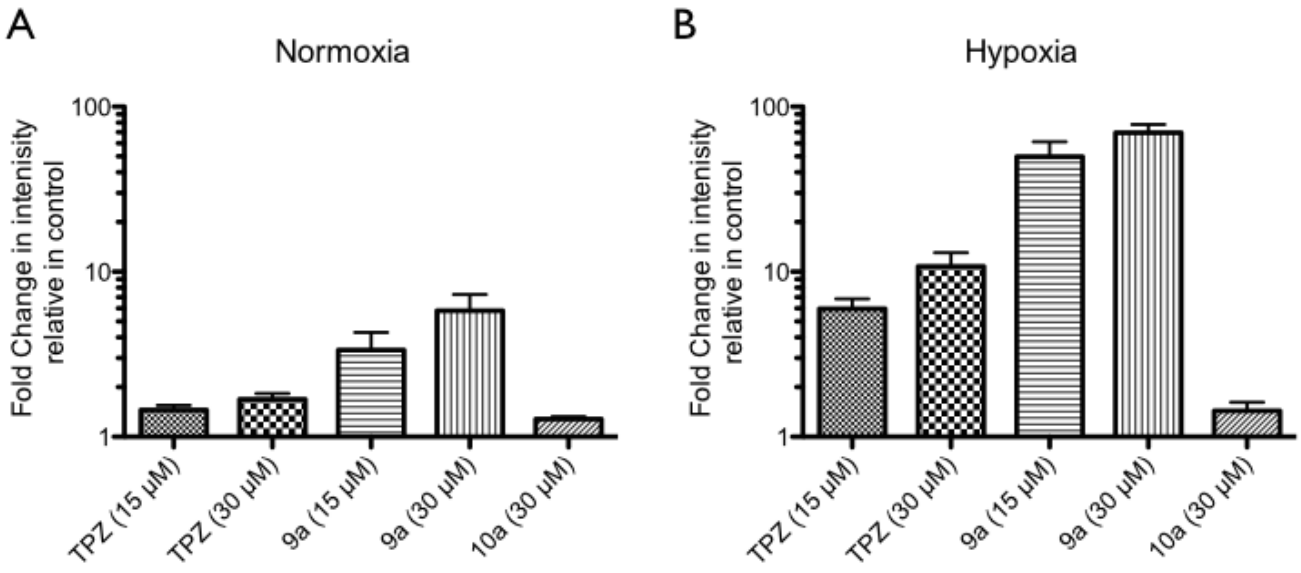

Fig. (4). Intracellular ROS changes of HCT-116 cells after treatment with TPZ, **9a** and **10a** in both normoxia and hypoxia. HCT-116 cells were treated with of TPZ, **9a** and **10a** for 18 hrs in both (A) normoxia and (B) hypoxia. All data were normalized on the basis of solvent control. Data were expressed as Mean ± SEM, n=3.

increase of ROS in hypoxia. No significant difference of ROS levels between normoxia and hypoxia was observed following treatment with compound **10a** (a dimeric 1,2,4-benzotriazine-1-oxide with an ethyl linker as a structurally and biologically comparative control), but the ROS level was 1.3 times that of the control medium. A comparison of the effects on ROS of exposure of HCT-116 cells to **9a** and TPZ in normoxia and hypoxia indicated that both **9a** and TPZ had dose-dependent effects, and the effect was stronger in hypoxia than in normoxia. Compound **9a** induced a higher ROS level than TPZ in both normoxia and hypoxia, but treatment with **10a** (as a structurally contrast control) negligibly increased ROS. These results indicated that the 1,2,4-benzotriazine-1,4-dioxide constituent was a structurally essential chromophore of compound **9a**, akin to that of TPZ, that causes selectively hypoxic DNA damage by enzymatic one-electron bioreductive activation, which has been described elsewhere [37-39].

One study has found that TPZ-induced cell apoptosis is accompanied by the activation of caspase 3/7 [40], so this investigation elucidated the important role of activated caspase 3/7 in mitochondria-dependent apoptosis [41] as well. The levels of activated caspase 3/7 in HCT-116 following treatment with TPZ, **9a** and **9b** at 30 μM were evaluated by flow cytometry (shown as Fig. **5**). In normoxia, TPZ, **9a** and **9b** at 30 μM had no apparent effect, but in hypoxia, they increased the levels of active caspase 3/7 in HCT-116 to about 41, 55 and 23% increase, respectively, relative to a solvent control (7%). These data suggest that TPZ- and TPZ derivatives-induced hypoxic cytotoxicity may involve mostly cell apoptosis, consistent with the evidence of an increase in the sub-G1 level in HCT-116.

A previous study found that TPZ induces a cellular response to damage to DNA. The expression of γ-H2AX (member X of the H2A histone family) is a biomarker of DNA damage, and the cleaved poly (ADP-ribose) polymerase (PARP) [42] is a biomarker of apoptosis in cancer cells in hypoxia as well [43]. The expression of γ-H2AX in HCT-116 cells in hypoxia after treatment with TPZ or **9a** at 30 μM was around 30% of that of the solvent control (only 4%). In normoxia, these treatments had no significant effect (Figs. **6A-B**). As presented in Figs. **6C-D**, the cleaved PARP of the cells in hypoxia another apoptosis marker is approximately 10% and 45% after treatment with TPZ and **9a**, respectively. No HCT-116 cells (0.1%) in normoxia exhibited both the expressed γ-H2AX and cleaved PARP after the treatment with TPZ or **9a** at 30 μM in the solvent control. However, in hypoxia, approximately 11 % of cells expressed the γ -H2AX and cleaved PARP following treatment with **9a** at 30 μM, the percentage of which was greater than that (1.9%) following treatment with TPZ at 30 μM (Fig. **6E**). These results reveal that TPZ induced DNA damage and cell apoptosis, consistent with the effects of TPZ on human cervical carcinoma cells [43], whereas, in hypoxia, **9a**-induced HCT-116 cell death by simultaneous DNA damage and PARP-cleaving activity reflected greater DNA damage- and mitochondria-dependent apoptosis than caused by TPZ, consistent with other reports [44-45].

3.2.4. In vitro Antangiogenic Activities

The tube formation of co-cultured HUVECs and fibroblasts was used to compare the anti-angiogenic activities of TPZ derivatives with those of TPZ and Suramin (a positive control of the kit) at two tested concentrations (2 and 20 μM).

Co-cultured HUVECs and fibroblasts were exposed to a commercial differentiation medium that contained 0.2 % DMSO, for only 11 days, and exhibited slightly increased tube areas, lengths, and numbers of joints over those in co-cultured cells that were incubated with medium alone (the same medium without DMSO). The selected compounds **7b**, **8g**, **9a** and **9b** were compared to TPZ in an anti-angiogenic activity assay and were found to have better selective hypoxic cytotoxicity than the other TPZ derivatives (Fig. **7**).

All of the selected compounds **7b**, **8g**, **9a** and **9b** at 20 μM had 80-90% inhibition of tube formation, whereas TPZ inhibited tube formation by 50% at 20 μM. At low concentration (2 μM), **9a** and **9b** significantly reduced the areas, lengths, paths and joints of tube formation by 70-80% and 45-50%. Other compounds inhibited tube formation to a lesser extent (**7b**, 10-22%; **8g**, 31-40%). These results indicated that TPZ and TPZ derivatives were potent anti-angiogenesis agents herein, and that **7b**, **8g, 9b** and especially **9a** exhibited stronger anti-angiogenic activity than TPZ. These results are consistent with previous studies that have shown that TPZ, a heteroaromatic di-N-oxide compound, inhibits angiogenesis

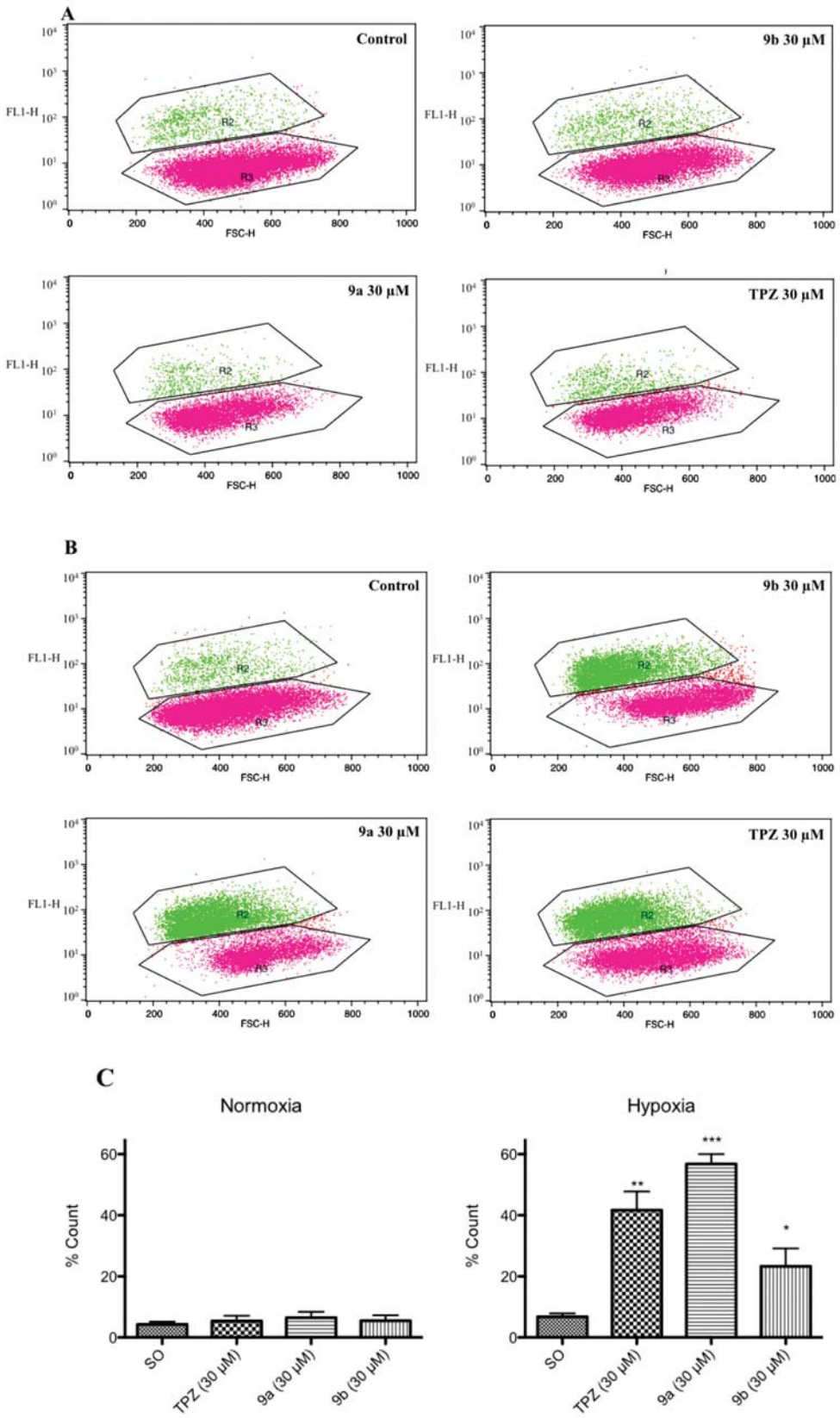

Fig. (5). TPZ and TPZ derivatives induced cellular activation of caspase 3/7 in hypoxia in HCT-116 cells. HCT-116 cells were treated with 30 µM concentration of TPZ, 9a and 9b in both normoxia and hypoxia. After 24 hours, cells were stained by ICT's FAM-FLICATM caspase-3/7 inhibitor kit and detected by flow cytometry. R2 area as cells which expressed active form of caspase 3/7, R3 as cell did not express active form of active caspase 3/7, (A) in normoxia, and (B) in hypoxia. (C) The level of active caspase 3/7 of HCT-116 cells after treatment with TPZ and TPZ derivatives in both normoxia and hypoxia. Data were shown as Mean ± SEM, n=3. Differences were considered statistically significant on the basis of solvent control as *, $p<0.05$; **, $p<0.01$; ***, $p<0.005$.

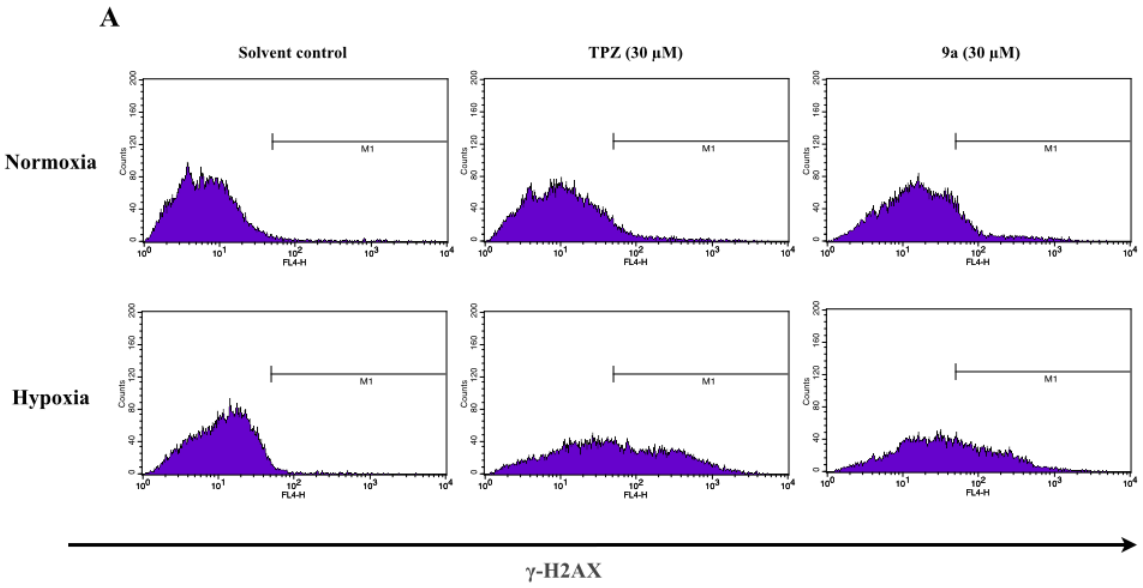
A
Solvent control
TPZ (30 μM)
9a (30 μM)
Normoxia
Hypoxia
M1
Counts
FL4-H
γ-H2AX

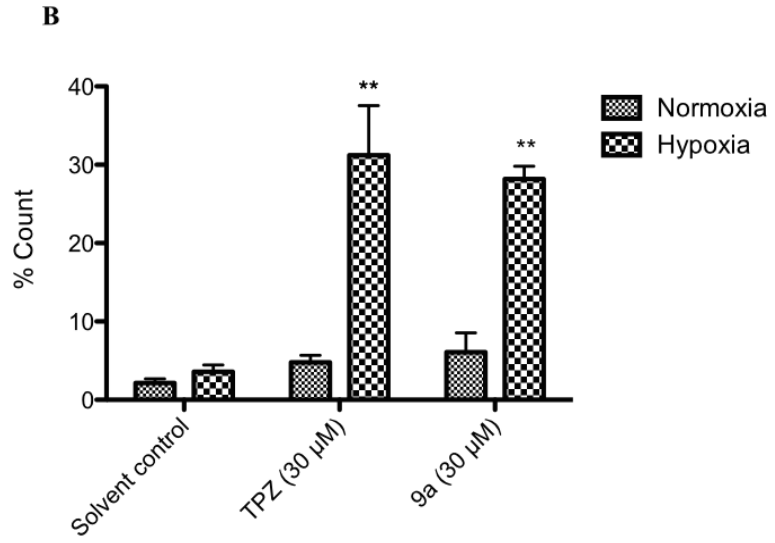
B
% Count
40
30
20
10
0
**
**
Normoxia
Hypoxia
Solvent control
TPZ (30 μM)
9a (30 μM)

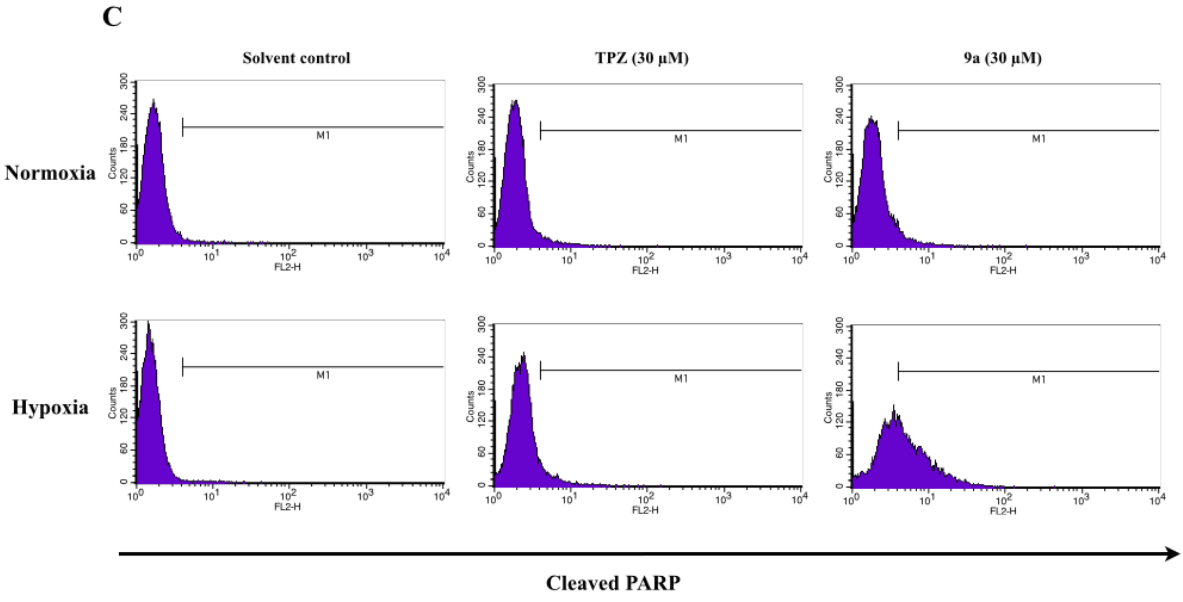
C
Solvent control
TPZ (30 μM)
9a (30 μM)
Normoxia
Hypoxia
M1
Counts
FL2-H
Cleaved PARP

Fig. (6). contd….

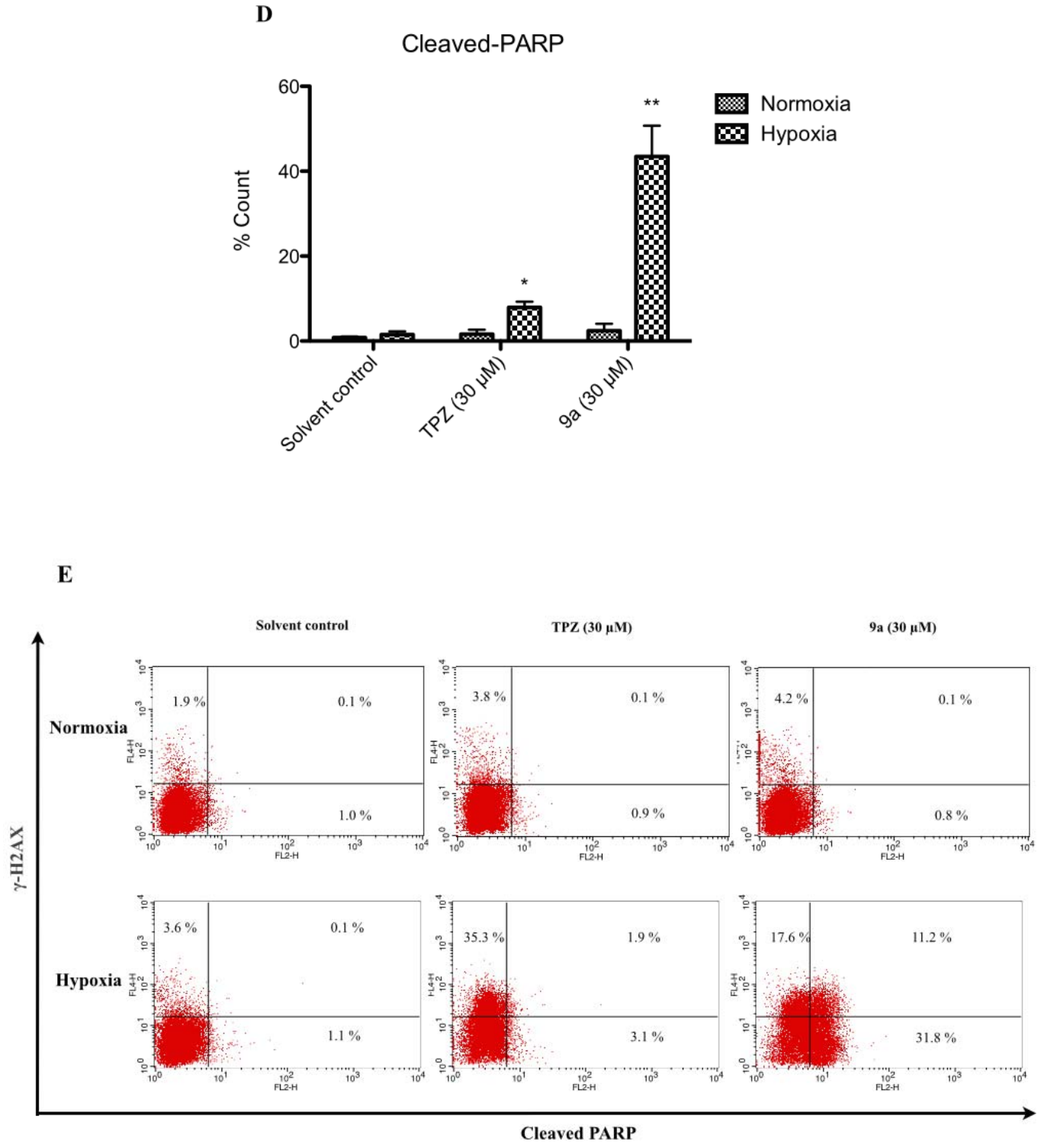

Fig. (6). Detection of level of γ-H2AX cleaved PARP in HCT-116 cells treated with TPZ and TPZ derivatives in both normoxia and hypoxia was conducted by flow cytometry. HCT-116 cells were treated with 30 μM of TPZ, **9a**, respectively, for 24 hrs in both normoxia and in hypoxia. (A) and (B) γ-H2AX, (C) and (D) cleaved-PARP, and (E) the dual parameter dots combining γ-H2AX and cleaved-PARP antibody showed DNA damage cells in upper half area, apoptotoic cells in right half area and aptoptoic cells with DNA damage in upper right quadrant. Data were shown as Mean ± SEM, n=3. Differences were considered statistically significant on the basis of solvent control as *, $p<0.05$; **, $p<0.01$.

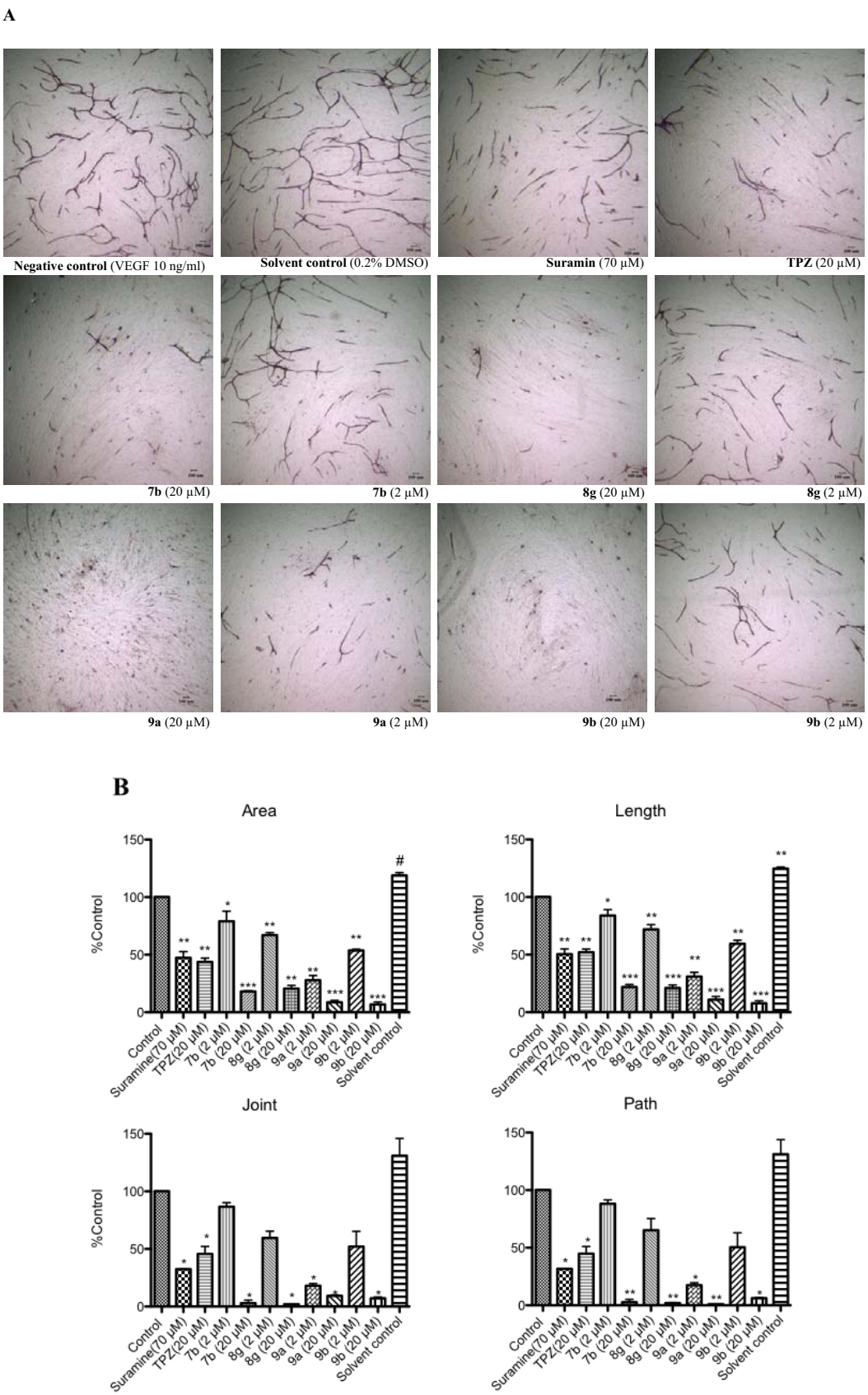

Fig. (7). Effect of TPZ and TPZ derivatives on tube formation by HUVECs and fibroblast co-cultured system. HUVECS were incubated with or without TPZ and TPZ derivatives at 2 and 20 μM, compared to Suramin (a positive control) and VEGF (a negative control) over 11 days. (**A**) Representative photographs of tube formation after treatment with TPZ and TPZ derivatives. (**B**) Areas, lengths, joints and paths of tube formation were measured by Angiogenesis Image Analyzer. Data was shown as Mean ± SEM, n=4. Differences were considered statistically significant on the basis of solvent control as *, $p<0.05$; **, $p<0.01$; ***, $p<0.005$.

in chick embryo chorioallantoic membrane (CAM) assay in normoxia [12, 14]. The details of the mechanism of the anti-angiogenic activities of TPZ and TPZ derivatives must still be further investigated.

4. CONCLUSION

In summary, 3-amino-1,2,4-benzotriazine-1,4-dioxide (tirapazamine, TPZ), a prodrug that is hypoxia-activated to a toxic radical, is an experimental phase III anticancer drug currently. A series of compounds were derived by structural modifications from TPZ (as a lead) in this work and their hypoxic cytotoxicity and selectivity were evaluated. TPZ derivatives, with a 3-amino-1,2,4-benzotriazine-1,4-dioxide core structure that incorporated alkyl linkers without or with the extended hetero moiety, 3-amino-1,2,4-benzotriazine-1-oxide, at the 3-position of TPZ, were synthesized.

According to the preferentially normoxic and hypoxic cytotoxicities against three cell lines, MCF-7, NCI-H460 and HCT-116, most of the synthesized compounds exhibited hypoxic cytotoxicity that was similar to or greater than that of TPZ. Compound **9a** exhibited hypoxic activity in the significant caspase 3/7-induced and G2/M arrest-mediated apoptosis, and its anti-angiogenic activity was stronger than that of TPZ. Compound **9a** was more potent than TPZ compound and should be preferred in detailed bioreductive anticancer studies from the bench to clinical.

CONFLICT OF INTEREST

The author(s) confirm that this article content has no conflict of interest.

ACKNOWLEDGEMENTS

The authors gratefully acknowledge the research grants supported from the Cheng-Hsin General Hospital (CHGH 97-63 & 98-68) and National Science Council (NSC 96-2320-B-016-001 & NSC96-2323-B016-005-MY3), Taiwan. Ted Knoy is appreciated for his editorial assistance.

LIST OF ABBREVIATIONS

CM-H_2DCFDA	=	5-(and-6)-Chloromethyl-2',7'-dichlorodi-hydrofluorescein diacetate, acetyl ester
DCM	=	Dichloromethane
γ-H2AX	=	H2A histone family, member X)
HUVEC	=	Human umbilical vein endothelial cell
HCR	=	Hypoxic cytotoxicity ratio
PARP	=	Poly (ADP-ribose) polymerase
PI	=	Propidium iodide
ROS	=	Reactive oxygen specie
TPZ	=	Tirapazamine
TFA	=	Trifluoroacetic acid
TFAA	=	Trifluoroacetic anhydride
TEA	=	Triethylamine

REFERENCES

[1] Gandara, D.R.; Lara, P.N.; Jr.; Goldberg, Z.; Le, Q.T.; Mack, P.C.; Lau, D.H.; Gumerlock, P.H. Tirapazamine: Prototype for a novel class of therapeutic agents targeting tumor hypoxia. *Semin. Oncol.,* **2002**, *29* (1 Suppl 4), 102-109.

[2] Zeman, E.M.; Brown, J.M.; Lemmon, M.J.; Hirst, V.K.; Lee, W.W. SR-4233: A new bioreductive agent with high selective toxicity for hypoxic mammalian cells. *Int. J. Radiat. Oncol. Biol. Phys.,* **1986**, *12* (7), 1239-1242.

[3] Lin, A.J.; Cosby, L.A.; Shansky, C.W.; Sartorelli, A.C. Potential bioreductive alkylating agents. 1. Benzoquinone derivatives. *J. Med. Chem.,* **1972**, *15* (12), 1247-1252.

[4] Lin, A.J.; Pardini, R.S.; Lillis, B.J.; Sartorelli, A.C. Potential bioreductive alkylating agents. 4. Inhibition of coenzyme Q enzyme systems by lipoidal benzoquinone and naphthoquinone derivatives. *J. Med. Chem.,* **1974**, *17* (7), 687-688.

[5] McKeown, S.R.; Cowen, R.L.; Williams, K.J. Bioreductive drugs: From concept to clinic. *Clin. Oncol. (R. Coll. Radiol.),* **2007**, *19* (6), 427-442.

[6] Brown, J.M.; Wilson, W.R. Exploiting tumour hypoxia in cancer treatment. *Nat. Rev. Cancer,* **2004**, *4* (6), 437-447.

[7] Kizaka-Kondoh, S.; Inoue, M.; Harada, H.; Hiraoka, M. Tumor hypoxia: A target for selective cancer therapy. *Cancer Sci.,* **2003**, *94* (12), 1021-1028.

[8] Denny, W.A. The role of hypoxia-activated prodrugs in cancer therapy. *Lancet Oncol.,* **2000**, *1* (1), 25-29.

[9] Walton, M.I.; Wolf, C.R.; Workman, P. Molecular enzymology of the reductive bioactivation of hypoxic cell cytotoxins. *Int. J. Radiat. Oncol. Biol. Phys.,* **1989**, *16* (4), 983-986.

[10] Peters, K.B.; Brown, J.M. Tirapazamine: A hypoxia-activated topoisomerase II poison. *Cancer Res.,* **2002**, *62* (18), 5248-5253.

[11] Chowdhury, G.; Junnotula, V.; Daniels, J.S.; Greenberg, M.M.; Gates, K.S. DNA strand damage product analysis provides evidence that the tumor cell-specific cytotoxin tirapazamine produces hydroxyl radical and acts as a surrogate for O(2). *J. Am. Chem. Soc.,* **2007**, *129* (42), 12870-1287.

[12] Nagasawa, H.; Mikamo, N.; Nakajima, Y.; Matsumoto, H.; Uto, Y.; Hori, H. Antiangiogenic hypoxic cytotoxin TX-402 inhibits hypoxia-inducible factor 1 signaling pathway. *Anticancer Res.,* **2003**, *23* (6a), 4427-4434.

[13] Zhang, J.; Cao, J.; Weng, Q.; Wu, R.; Yan, Y.; Jing, H.; Zhu, H.; He, Q.; Yang, B. Suppression of hypoxia-inducible factor 1alpha (HIF-1alpha) by tirapazamine is dependent on eIF2alpha phosphorylation rather than the mTORC1/4E-BP1 pathway. *PLoS One,* **2010**, *5* (11), e13910.

[14] Nagasawa, H.; Yamashita, M.; Mikamo, N.; Shimamura, M.; Oka, S.; Uto, Y.; Hori, H. Design, synthesis and biological activities of antiangiogenic hypoxic cytotoxin, triazine-N-oxide derivatives. *Comp. Biochem. Physiol. A. Mol. Integr. Physiol.,* **2002**, *132* (1), 33-40.

[15] Siim, B.G.; Van Zijl, P.L.; Brown, J.M. Tirapazamine-induced DNA damage measured using the comet assay correlates with cytotoxicity towards hypoxic tumour cells *in vitro*. *Br. J. Cancer,* **1996**, *73* (8), 952-960.

[16] Delahoussaye, Y.M.; Hay, M.P.; Pruijn, F.B.; Denny, W.A.; Brown, J.M. Improved potency of the hypoxic cytotoxin tirapazamine by DNA-targeting. *Biochem. Pharmacol.,* **2003**, *65* (11), 1807-1815.

[17] Peters, K.B.; Brown, J.M. Tirapazamine: A hypoxia-activated topoisomerase II poison. *Cancer Res.,* **2002**, *62* (18), 5248-5253.

[18] Xia, Q.; Zhang, L.; Zhang, J.; Sheng, R.; Yang, B.; He, Q.; Hu, Y. Synthesis, hypoxia-selective cytotoxicity of new 3-amino-1,2,4-benzotriazine-1,4-dioxide derivatives. *Eur. J. Med. Chem.,* **2011**, *46* (3), 919-926.

[19] Hay, M.P.; Gamage, S.A.; Kovacs, M.S.; Pruijn, F.B.; Anderson, R.F.; Patterson, A.V.; Wilson, W.R.; Brown, J.M.; Denny, W.A. Structure-activity relationships of 1,2,4-benzotriazine 1,4-dioxides as hypoxia-selective analogues of tirapazamine. *J. Med. Chem.,* **2003**, *46* (1), 169-182.

[20] Shinde, S.S.; Anderson, R.F.; Hay, M.P.; Gamage, S.A.; Denny, W.A. Oxidation of 2-deoxyribose by benzotriazinyl radicals of antitumor 3-amino-1,2,4-benzotriazine 1,4-dioxides. *J. Am. Chem. Soc.,* **2004**, *126* (25), 7865-7874.

[21] Rischin, D.; Peters, L.J.; O'Sullivan, B.; Giralt, J.; Fisher, R.; Yuen, K.; Trotti, A.; Bernier, J.; Bourhis, J.; Ringash, J.; Henke, M.; Kenny, L. Tirapazamine, cisplatin, and radiation versus cisplatin and radiation for advanced squamous cell carcinoma of the head and neck (TROG 02.02, HeadSTART): A phase III trial of the Trans-Tasman Radiation Oncology Group. *J. Clin. Oncol.,* **2010**, *28* (18), 2989-2995.

[22] Reddy, S.B.; Williamson, S.K. Tirapazamine: A novel agent targeting hypoxic tumor cells. *Expert. Opin. Investig. Drugs,* **2009**, *18* (1), 77-87.

[23] Hay, M.P.; Pruijn, F.B.; Gamage, S.A.; Liyanage, H.D.; Kovacs, M.S.; Patterson, A.V.; Wilson, W.R.; Brown, J.M.; Denny, W.A.

DNA-targeted 1,2,4-benzotriazine 1,4-dioxides: Potent analogues of the hypoxia-selective cytotoxin tirapazamine. *J. Med. Chem.,* **2004**, *47* (2), 475-488.

[24] Huxham, L.A.; Kyle, A.H.; Baker, J.H.; McNicol, K.L.; Minchinton, A.I. Tirapazamine causes vascular dysfunction in HCT-116 tumour xenografts. *Radiother. Oncol.,* **2006**, *78* (2), 138-145.

[25] Huxham, L.A.; Kyle, A.H.; Baker, J.H.; McNicol, K.L.; Minchinton, A.I. Exploring vascular dysfunction caused by tirapazamine. *Microvasc. Res.,* **2008**, *75* (2), 247-255.

[26] Baker, J.H.; Kyle, A.H.; Bartels, K.L.; Methot, S.P.; Flanagan, E.J.; Balbirnie, A.; Cran, J.D.; Minchinton, A.I. Targeting the tumour vasculature: Exploitation of low oxygenation and sensitivity to NOS inhibition by treatment with a hypoxic cytotoxin. *PLoS One,* **2013**, *8* (10), e76832.

[27] Nakashima, H.; Uto, Y.; Nakata, E.; Nagasawa, H.; Ikkyu, K.; Hiraoka, N.; Nakashima, K.; Sasaki, Y.; Sugimoto, H.; Shiro, Y.; Hashimoto, T.; Okamoto, Y.; Asakawa, Y.; Hori, H. Synthesis and biological activity of 1-methyl-tryptophan-tirapazamine hybrids as hypoxia-targeting indoleamine 2,3-dioxygenase inhibitors. *Bioorg. Med. Chem.,* **2008**, *16* (18), 8661-8669.

[28] Brown, J.M.; Denny, D.A.; Gamage, S.A.; Hay, M.P.; Hicks, K.O.; Pruijin, F.B.; W.R. Wilson *DNA-Target benxotriazine 1,4-dioxides and their use in cancer therapy*. Patent WO2004026846 A1, (2004).

[29] Pruijn, F.B.; Sturman, J.R.; Liyanage, H.D.; Hicks, K.O.; Hay, M.P.; Wilson, W.R. Extravascular transport of drugs in tumor tissue: Effect of lipophilicity on diffusion of tirapazamine analogues in multicellular layer cultures. *J. Med. Chem.,* **2005**, *48* (4), 1079-1087.

[30] Siim, B.G.; Hicks, K.O.; Pullen, S.M.; Van Zijl, P.L.; Denny, W.A.; Wilson, W.R. Comparison of aromatic and tertiary amine N-oxides of acridine DNA intercalators as bioreductive drugs. Cytotoxicity, DNA binding, cellular uptake, and metabolism. *Biochem. Pharmacol.,* **2000**, *60* (7), 969-978.

[31] Fuchs, T.; Chowdhury, G.; Barnes, C.L.; Gates, K.S. 3-Amino-1,2,4-benzotriazine 4-oxide: Characterization of a new metabolite arising from bioreductive processing of the antitumor agent 3-amino-1,2,4-benzotriazine 1,4-dioxide (tirapazamine). *J. Org. Chem.,* **2001**, *66* (1), 107-114.

[32] Pchalek, K.; Hay, M.P. Stille coupling reactions in the synthesis of hypoxia-selective 3-alkyl-1,2,4-benzotriazine 1,4-dioxide anticancer agents. *J. Org. Chem.,* **2006**, *71* (17), 6530-6535.

[33] Hong, B.; Lui, V.W.; Hui, E.P.; Ng, M.H.; Cheng, S.H.; Sung, F.L.; Tsang, C.M.; Tsao, S.W.; Chan, A.T. Hypoxia-targeting by tirapazamine (TPZ) induces preferential growth inhibition of nasopharyngeal carcinoma cells with Chk1/2 activation. *Invest. New Drugs,* **2011**, *29* (3), 401-410.

[34] Jiang, F.; Yang, B.; Fan, L.; He, Q.; Hu, Y. Synthesis and hypoxic-cytotoxic activity of some 3-amino-1,2,4-benzotriazine-1,4-dioxide derivatives. *Bioorg. Med. Chem. Lett.,* **2006**, *16* (16), 4209-4213.

[35] Shinde, S.S.; Hay, M.P.; Patterson, A.V.; Denny, W.A.; Anderson, R.F. Spin trapping of radicals other than the *OH radical upon reduction of the anticancer agent tirapazamine by cytochrome P450 reductase. *J. Am. Chem. Soc.,* **2009**, *131* (40), 14220-1422.

[36] Anderson, R.F.; Shinde, S.S.; Hay, M.P.; Gamage, S.A.; Denny, W.A. Radical properties governing the hypoxia-selective cytotoxicity of antitumor 3-amino-1,2,4-benzotriazine 1,4-dioxides. *Org. Biomol. Chem.,* **2005**, *3* (11), 2167-2174.

[37] Brown, J.M. SR 4233 (tirapazamine): A new anticancer drug exploiting hypoxia in solid tumours. *Br. J. Cancer,* **1993**, *67* (6), 1163-1170.

[38] Siim, B.G.; Van Zijl, P.L.; Brown, J.M. Tirapazamine-induced DNA damage measured using the comet assay correlates with cytotoxicity towards hypoxic tumour cells *in vitro*. *Br. J. Cancer,* **1996**, *73* (8), 952-960.

[39] Daniels, J.S. Photochemical DNA cleavage by the antitumor agent 3-Amino-1,2,4-benzotriazine 1,4-dioxide (tirapazamine, WIN 59075, SR4233). *J. Org. Chem.,* **1998**, *63*, 10027-10030.

[40] Mayes, P.A.; Dolloff, N.G.; Daniel, C.J.; Liu, J.J.; Hart, L.S.; Kuribayashi, K.; Allen, J.E.; Jee, D.I.; Dorsey, J.F.; Liu, Y.Y.; Dicker, D.T.; Brown, J.M.; Furth, E.E.; Klein, P.S.; Sears, R.C.; El-Deiry, W.S. Overcoming hypoxia-induced apoptotic resistance through combinatorial inhibition of GSK-3beta and CDK1. *Cancer Res.,* **2011**, *71* (15), 5265-5275.

[41] Lakhani, S.A.; Masud, A.; Kuida, K.; Porter, G.A., JR.; Booth, C.J.; Mehal, W.Z.; Inayat, I.; Flavell, R.A. Caspases 3 and 7: Key mediators of mitochondrial events of apoptosis. *Science,* **2006**, *311* (5762), 847-851.

[42] Kim, S.B.; Chae, G.W.; Lee, J.; Park, J.; Tak, H.; Chung, J.H.; Park, T.G.; Ahn, J.K.; Joe, C.O. Activated Notch1 interacts with p53 to inhibit its phosphorylation and transactivation. *Cell Death Differ.,* **2007**, *14* (5), 982-991.

[43] Olive, P.L.; Banath, J.P.; Sinnott, L.T. Phosphorylated histone H2AX in spheroids, tumors, and tissues of mice exposed to etoposide and 3-amino-1,2,4-benzotriazine-1,3-dioxide. *Cancer Res.,* **2004**, *64* (15), 5363-5369.

[44] Wouters, B.G.; Delahoussaye, Y.M.; Evans, J.W.; Birrell, G.W.; Dorie, M.J.; Wang, J.; MacDermed, D.; Chiu, R.K.; Brown, J.M. Mitochondrial dysfunction after aerobic exposure to the hypoxic cytotoxin tirapazamine. *Cancer Res.,* **2001**, *61* (1), 145-152.

[45] Park, D.; Dilda, P.J. Mitochondria as targets in angiogenesis inhibition. *Mol. Aspects. Med.,* **2010**, *31* (1), 113-131.

Received: August 12, 2014 Revised: September 25, 2014 Accepted: September 27, 2014